

Atmospheric Rivers in the Eastern and Midwestern United States Associated with Baroclinic Waves

Travis Allen O'Brien¹, Burlen Loring², Amanda Dufek³, Mohammad Rubaiat Islam¹, Diya Kamnani¹, Kwesi Twentwewa Quagraine¹, and Cody Kirkpatrick¹

¹Indiana University Bloomington

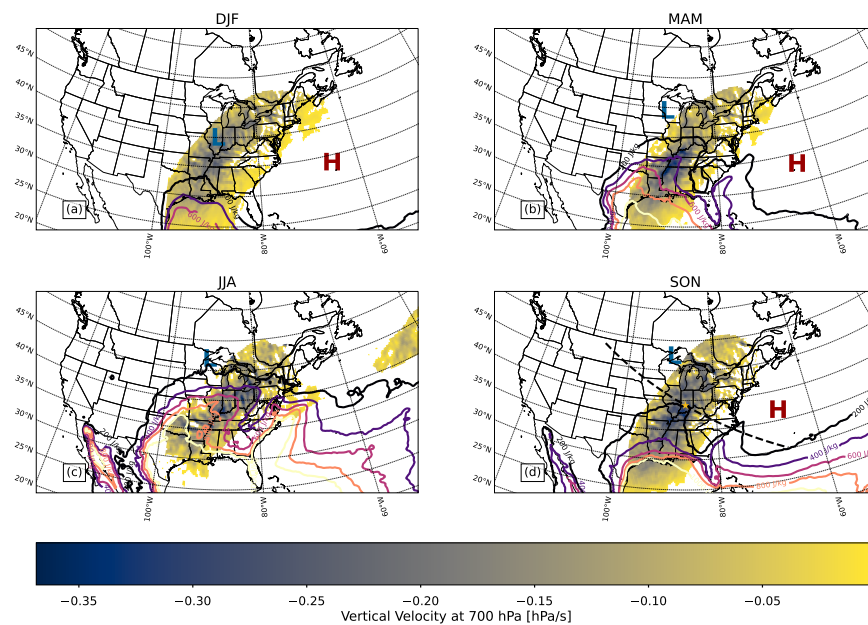
²Lawrence Berkeley Lab

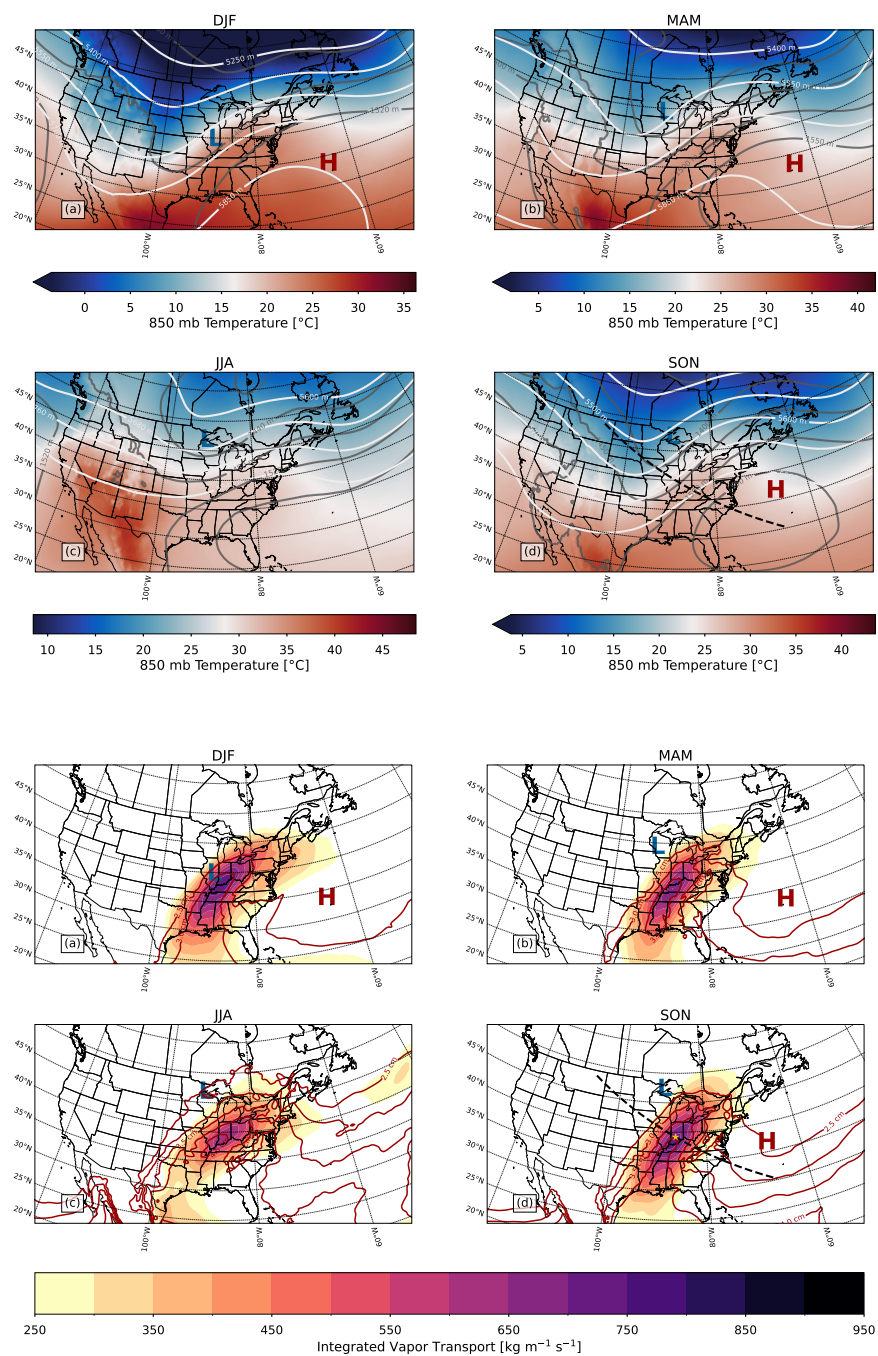
³Lawrence Berkeley National Lab

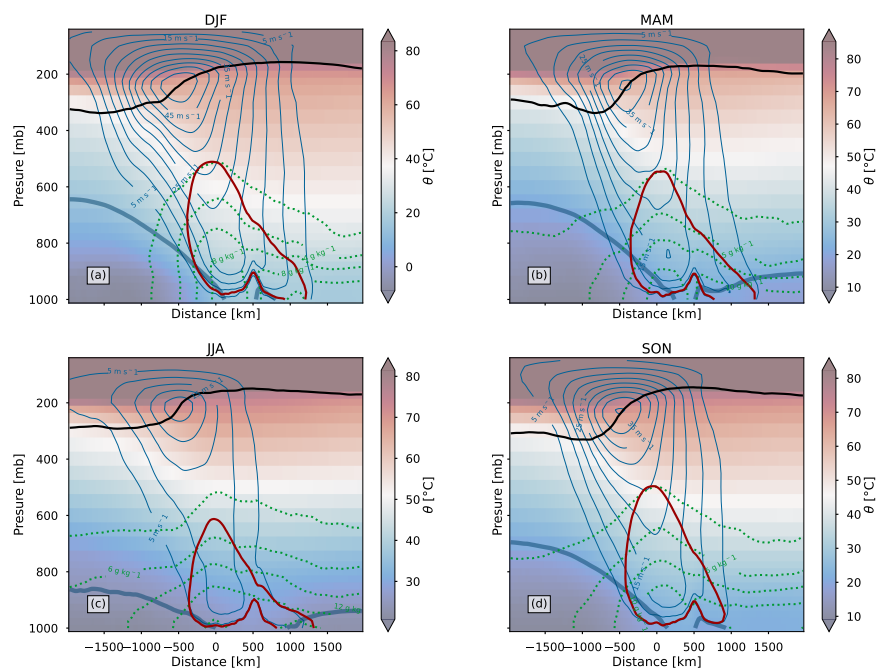
November 14, 2023

Abstract

Atmospheric rivers (ARs) significantly impact the hydrological cycle and associated extremes in western continental regions. Recent studies suggest ARs also influence water resources and extremes in continental interiors. AR detection tools indicate that AR conditions are relatively frequent in areas east of the Rocky Mountains. The origin of these ARs, whether from synoptic-scale waves or mesoscale processes, is unclear. This study uses meteorological composite maps and transects of AR conditions during the four seasons. The analysis reveals that ARs east of the Rockies are associated with a long-wave baroclinic Rossby wave. This result demonstrates that eastern and midwestern ARs are dynamically similar to their western coastal counterparts, though mechanisms for vertical moisture flux differ between the two. These findings provide a foundation for understanding future climate change and ARs in this region and offer new methods for evaluating climate model simulations.







Atmospheric Rivers in the Eastern and Midwestern United States Associated with Baroclinic Waves

Travis A. O'Brien,^{1,2}Burlen Loring,³Amanda Dufek,⁴Mohammad Rubaiat Islam,¹Diya Kamnani,¹Kwesi Quagraine,¹Cody Kirkpatrick¹

¹Department of Earth and Atmospheric Sciences, Indiana University, Bloomington, IN, USA

²Climate and Ecosystem Sciences Division, Lawrence Berkeley National Lab, Berkeley, CA, USA

³Computational Research Division, Lawrence Berkeley National Lab, Berkeley, CA, USA

⁴National Energy Research Supercomputing Center, Lawrence Berkeley National Lab, Berkeley, CA, USA

Key Points:

- Atmospheric rivers (ARs) east of the Rockies are associated with baroclinic waves
- Western coastal ARs and eastern/midwest ARs are dynamically similar
- Synoptic-scale uplift, combined with convective instability, provide efficient mechanisms for generating precipitation

Abstract

Atmospheric rivers (ARs) significantly impact the hydrological cycle and associated extremes in western continental regions. Recent studies suggest ARs also influence water resources and extremes in continental interiors. AR detection tools indicate that AR conditions are relatively frequent in areas east of the Rocky Mountains. The origin of these ARs, whether from synoptic-scale waves or mesoscale processes, is unclear. This study uses meteorological composite maps and transects of AR conditions during the four seasons. The analysis reveals that ARs east of the Rockies are associated with a long-wave baroclinic Rossby wave. This result demonstrates that eastern and midwestern ARs are dynamically similar to their western coastal counterparts, though mechanisms for vertical moisture flux differ between the two. These findings provide a foundation for understanding future climate change and ARs in this region and offer new methods for evaluating climate model simulations.

Plain Language Summary

Atmospheric rivers (ARs) are a weather pattern that brings high amounts of atmospheric water and winds in a relatively narrow region. ARs are typically considered a ‘west coast’ phenomenon, largely because the majority of the scientific research on ARs has focused on ARs in western coastal regions: particularly the western United States. ARs occur in continental interiors, but there has been some debate about whether these ARs represent the same type of weather as those in western coastal regions.

This paper uses two objective methods for identifying ARs and finds times when ARs are present in two locations in the eastern half of the United States: Bloomington, IN and Washington, DC. Examination of weather conditions during these AR times shows remarkable similarity to conditions associated with west coast ARs. This gives strong evidence that ARs do occur in the eastern half of the United States. This result is important because it suggests that ARs may be important for water resources and extreme weather in the eastern half of the United States, just as they are in the western United States. This result also suggests that ARs may be important for water resources and extremes in other continental interiors.

1 Introduction

Atmospheric rivers (AR) are widely recognized as being important for water resources and impacts in western coastal zones, with nearly 30 years of research establishing their meteorological context (Newell et al., 1992; Newell & Zhu, 1994; Zhu & Newell, 1994; Neiman et al., 2002; Ralph et al., 2004, 2005), demonstrating their importance for the hydrological cycle at global and regional scales (Zhu & Newell, 1998; Bao et al., 2006; Neiman, Ralph, Wick, Lundquist, & Dettinger, 2008; Neiman, Ralph, Wick, Kuo, et al., 2008; Strong & Magnusdottir, 2008a, 2008b; Knippertz & Wernli, 2010; Viale & Nuñez, 2011; Guan et al., 2011; Newman et al., 2012; Cordeira et al., 2013; Ryoo et al., 2013; Sodemann & Stohl, 2013; Rutz et al., 2014; Dacre et al., 2015; Guan & Waliser, 2015; L. M. Smith & Stechmann, 2017; Eiras-Barca et al., 2018; Z. Zhang et al., 2019; Guo et al., 2020, e.g.), and establishing their connection with extreme precipitation and impacts (Ralph et al., 2006; Stohl et al., 2008; Leung & Qian, 2009; Dettinger, 2011; Ralph & Dettinger, 2012; Lavers et al., 2012; Warner et al., 2012; Ralph et al., 2013; Gimeno et al., 2016; Waliser & Guan, 2017; Ralph, Wilson, et al., 2019; Griffith et al., 2020). AR research has expanded dramatically in the last 10 years, with numerous new papers on their qualitative and quantitative definition (see e.g., Ralph et al., 2018; Ralph, Rutz, et al., 2019; Shields et al., 2018; Rutz et al., 2019; Lora et al., 2020; O’Brien et al., 2020; Collow et al., 2022, and references therein), AR variability and change (Dettinger, 2011; Gao et al., 2015; Payne & Magnusdottir, 2015; Warner et al., 2015; Hagos et al., 2016; Mundhenk et al., 2016; Gershunov et al., 2017; Lora et al., 2017; Warner & Mass, 2017;

Dong et al., 2018; Espinoza et al., 2018; Mundhenk et al., 2018; Zhou et al., 2018; Zhou & Kim, 2018; Cao et al., 2020; McClenney et al., 2020; Payne et al., 2020; Rhoades et al., 2020; O'Brien et al., 2021; Reid et al., 2021; Zhou et al., 2021; Ma & Chen, 2022), and AR forecasting (Lavers, Pappenberger, et al., 2016; Lavers, Waliser, et al., 2016; DeFlo-rio et al., 2018, 2019; Lavers et al., 2020; Cao et al., 2021; Zheng et al., 2021). The list of topics and citations here is meant to be illustrative rather than exhaustive; there are now hundreds of atmospheric river papers in the literature.

The vast majority of papers in the AR literature are focused on studies of west-ern coastal zones, with most centered specifically on the United States West Coast where much of the early research on ARs was directed. That said, there is an increasing recog-nition that atmospheric rivers are also important in other regions, such as continental interiors and polar regions (Gorodetskaya et al., 2014; Wille et al., 2019; Nash et al., 2018), the interiors of Australia and China (Liang et al., 2020; Rauber et al., 2020; Y. Xu et al., 2020; L. Xu et al., 2020; H. Zhang et al., 2020; Nash et al., 2021; Reid et al., 2021), the Middle East and North Africa (Massoud et al., 2020), and the interior of the United States east of the Rocky Mountains (Dirmeyer & Kinter, 2009, 2010; Moore et al., 2012; Slinskey et al., 2020).

For two specific examples, significant flooding events have occurred in the midwest-ern United States in association with atmospheric rivers: one in Nashville, Tennessee on May 1–2, 2010 (Moore et al., 2012) and one in Bloomington, Indiana on June 18–19, 2021. The Bloomington flood was a 100-year event in which multiple rain gauges recorded over 15 cm (6 in) of rainfall in a 24-hour period. Analysis of the associated meteorology (and use of an objective AR detection tool; see Section 2) shows that the flood was associ-ated with the combination of an AR, a cold frontal zone (as indicated by a region of lo-cal maximum gradient in 850 hPa temperatures), and a mesoscale convective complex (as indicated by a large coherent zone for which cloud brightness temperatures are lower than the 225 K threshold determined by Feng et al. (2018)); see Figure S1.

Several studies (Lavers & Villarini, 2013; Mahoney et al., 2016; Nakamura et al., 2013; Nayak et al., 2016; Slinskey et al., 2020) demonstrate the importance of ARs for extreme precipitation in areas of the United States (US) east of the Rocky Mountains. However, some literature (Dirmeyer & Kinter, 2010; Gimeno et al., 2010, 2016) presents a hypothesis that midwestern and eastern (hereafter ‘eastern’ for brevity) US ARs are fundamentally different from their west coast counterparts, in that they are a manifes-tation of the Great Plains Low Level Jet (GPLLJ).

A counter-hypothesis is that these eastern US ARs, like their west coast counter-parts, are driven by synoptic-scale eddies; i.e., they are primarily associated with baro-clinic Rossby waves. Both hypotheses are testable. The Great Plains LLJ is thought to be regulated by an inertial oscillation modulated by a consistent meridional buoyancy gradient, rather than synoptic-scale waves (Gebauer & Shapiro, 2019). If baroclinic waves are the primary driver, then we would expect the signatures of these midlatitude sys-tems to be evident in meteorological composites of times that satisfy AR conditions in the central US. Indeed, (Lavers & Villarini, 2013) show composites of mean sea-level pres-sure suggesting the influence of synoptic-scale dynamics.

Using composites of reanalysis data, we find support for the baroclinic Rossby wave hypothesis. Our results show that eastern US ARs are dynamically similar to their well-studied west coast counterparts in terms of their association with baroclinic waves.

2 Methods

We detect ARs using the Toolkit for Extreme Climate Analysis (TECA) Bayesian Atmospheric River Detector (`teca_bard_v1.0.1`) application, which simultaneously uses 1,024 equally plausible AR detectors to detect ARs with uncertainty quantification (O’Brien

et al., 2020). As in O’Brien et al. (2020), we apply `teca_bard_v1.0.1` to six-hourly MERRA-2 reanalysis output (Gelaro et al., 2017) spanning January 1, 1980 through December 31, 2021 (376,944 timesteps). For the analyses shown in Figures 1, 2, and 3, we identify high-confidence AR conditions over Bloomington, IN when the AR probability from `teca_bard_v1.0.1` is 100%. This results in 1,089 AR timesteps total, with 219 in DJF, 172 in MAM, 243 in JJA, and 455 in SON.

We test the sensitivity of our results to choice of ARDT and to location by repeating the entire analysis with a more permissive ARDT, `guan_waliser_v2` (Guan & Waliser, 2015), and by repeating the entire analysis with `teca_bard_v1.0.1` in a different location in the eastern United States: Washington, DC. The `guan_waliser_v2` data come from the Atmospheric River Tracking Method Intercomparison Project (ARTMIP) Tier 1 database (Shields et al., 2018), which spans the years 1980-2017. Results of these sensitivity studies are provided in Supplemental Information (Figures S2–S9). The `guan_waliser_v2` ARDT detects nearly 10 times more timesteps with AR conditions occurring over Bloomington, IN: 12,400 total, 2,925 in DJF, 3,379 in MAM, 2,754 in JJA, and 3,342 in SON. The `teca_bard_v1.0.1` ARDT detects a total of 1,548 timesteps with AR conditions over Washington, D.C., with a similar distribution among seasons.

We generate composites of various meteorological quantities during the Bloomington, IN AR timesteps, as indicated above, within each season using the ERA5 reanalysis (Hersbach et al., 2020; European Centre for Medium-Range Weather Forecasts, 2019). Note that the AR timesteps come from MERRA-2 due to our use of the ARTMIP dataset, but the meteorological composites come from ERA5. We utilize geopotential height, temperature, integrated vapor transport, integrated water vapor, winds, potential vorticity, vertical velocity, and mean sea-level pressure. Composites are generated using the `teca_temporal_reduction` application available within TECA (Loring et al., 2022; Prabhat et al., 2015). In the composite maps (Figures 1–4), we determine the location of surface low and high-pressure regions by finding the location of minimum sea-level pressure in the region bounded by the box (100 °W, 35 °N), (80 °W, 50 °N) for the low and by finding the location of maximum sea-level pressure in the region bounded by the box (85 °W, 25 °N), (55 °W, 45 °N) for the high. These search regions were determined by visual inspection of the composites. A local minimum sea-level pressure is found for all four seasons, and a local maximum sea-level pressure is found for all seasons except JJA.

In the composite transect in Section 3, the frontal zone locations are determined by (1) finding the location of the maximum 1000 mb potential temperature gradient in each season, and by (2) contouring the isentrope corresponding to the 1000 mb potential temperature at that location. The dynamic tropopause in Figure 3a–d is determined by the location of the 2 PVU potential vorticity contour. Cross-transect winds are calculated by taking the dot product of the transect-normal vector and the winds, and cross-transect moisture transport is calculated as the cross-transect wind times specific humidity.

3 Results

Figure 1 shows composites of integrated vapor transport (IVT; vertically integrated horizontal moisture flux), total column water vapor (IWV), and the locations of surface lows and highs for all four seasons. The IVT and IWV fields show the distinctive signature of atmospheric river conditions, namely a long, narrow band of high water vapor transport co-located with high precipitable water content. In all four seasons, a surface low is present to the northwest of the central AR zone (southern Indiana), and a surface high is present over the Atlantic Ocean in all seasons except JJA which instead shows a broad ridge pattern over the region. The ARs occur within a region of high surface pressure gradient between these low and high-pressure regions.

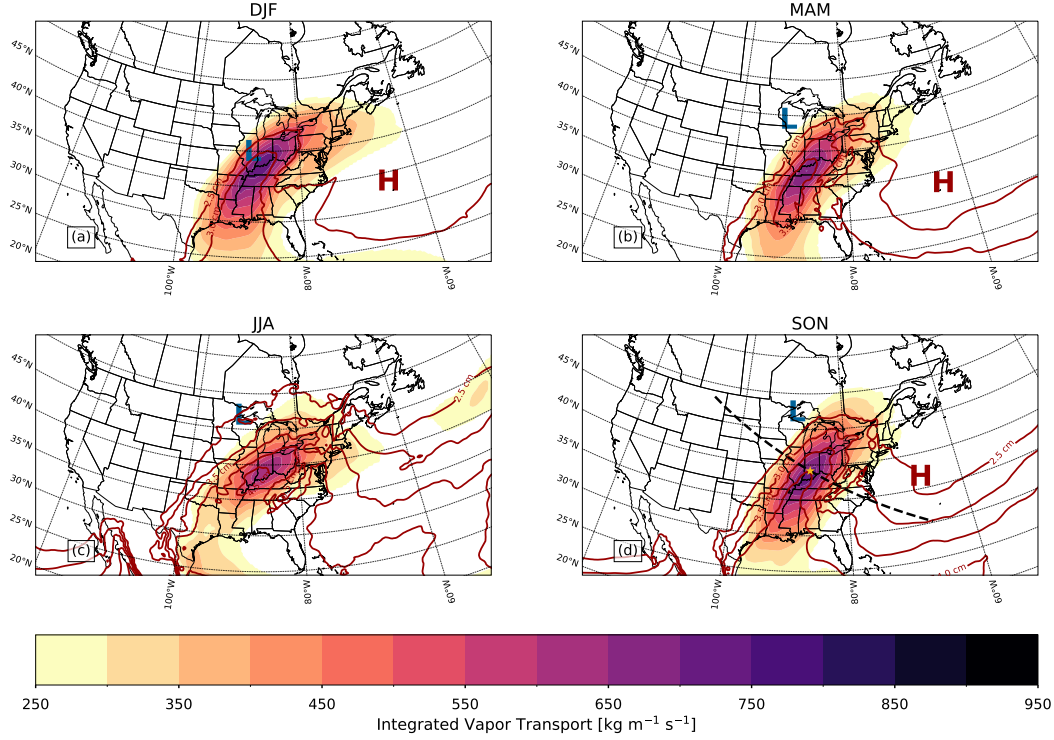


Figure 1. Composite maps of integrated vapor transport (shading), total column water vapor (red contours), and surface low and high pressures (L and H symbols) for AR conditions over Bloomington, IN in (a) DJF, (b) MAM, (c) JJA, and (d) SON. The dashed black curve in (d) shows the location of the transect in Figure 3, and the yellow star shows the location of Bloomington, IN.

To put the AR conditions in a synoptic context, Figure 2 shows composites of 850 mb potential temperature, 850 mb heights, 500 mb heights, and the same low/high-pressure regions shown in Figure 1. The upper-level heights show the clear presence of a longwave trough, with the mean trough axis 500–1500 km to the west of the AR region in all four seasons and a ridge to the east, such that upper-level geostrophic winds are southwesterly over the AR region. The lower-level heights also show a clear longwave pattern, with a phase offset of several hundred kilometers to the east of the upper-level trough axis in all four seasons. The surface low sits within, or just to the east of, the low-level trough.

The 850-mb potential temperature field also shows signs of a wave-like pattern, with a mean temperature gradient west of the AR region that would be associated with cold frontal zones, and signs of a warm frontal zone to the east of the AR region. Mean temperature features that could be correlated with fronts are much less well-defined in JJA, consistent with the weaker temperature gradients expected in Northern Hemisphere summer in midlatitudes.

In all four seasons, a mean upper-level trough exists west of the study region. If we were to treat each of the composite maps as representative of a typical event in that season, then this trough location indicates that the cyclonic vorticity associated with the trough is being advected eastward over the study region. The intensification of the winds with height (shown more clearly in Figure 3) indicates that the cyclonic vorticity advection increases with height. Such differential cyclonic vorticity advection is consistent with quasigeostrophic forcing favoring ascent over the region (Holton, 2004).

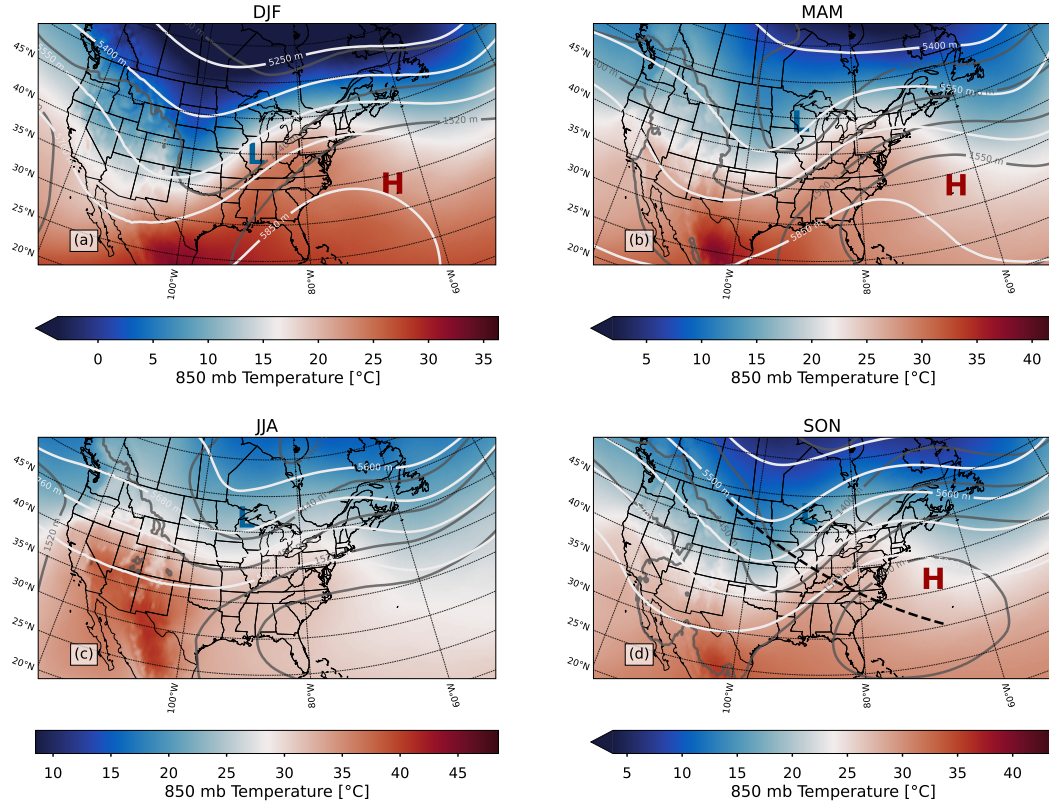


Figure 2. Composite maps of 850 mb potential temperature (shading), 850 mb heights (dark gray contours), 500 mb heights (light gray contours), and surface low and high pressures (L and H symbols) for AR conditions over Bloomington, IN in (a) DJF, (b) MAM, (c) JJA, and (d) SON. The dashed black curve in (d) shows the location of the transect in Figure 3.

The transect composites (Figure 3; see Figure 2d for the trace of the transect) show the presence of an upper-level jet with a maximum to the northwest of the AR region (to the left of 0 in the transects) and just below the tropopause in all four seasons. The upper-level jet is strongest in DJF but weakest in JJA, and exhibits a westward tilt in all four seasons, with relatively strong winds from the upper levels down toward the surface. All four seasons also exhibit a relative maximum in wind speed near the surface approximately 200-300 km to the southeast (right of 0 in the transects), which indicates the presence of a low-level jet. These winds are thermally-forced, as indicated by composites generated using geostrophic winds instead of the full wind field; these composites (not shown) are essentially identical to those in Figure 2. The potential temperature field shows indications of a cold frontal region, with a dome of relatively cold air extending from the surface up to about 300 hPa to the northwest (left of 0). The actual values of potential temperature vary according to season, but the general structure of the frontal region is consistent. The maximum gradient in 1000 mb temperatures is reached at or near the AR region, indicating that individual AR events may be associated with an impinging cold front.

Near-surface specific humidity (green dashed lines in Figure 3) reaches at least 10 g kg^{-1} in all seasons, with highest values primarily to the southeast of the AR region. The combination of high specific humidity, increased winds associated with the upper-level jet, and increased winds in the lower atmosphere result in high moisture transport directly over the AR region, consistent with the high IVT values shown in Figure 1. The

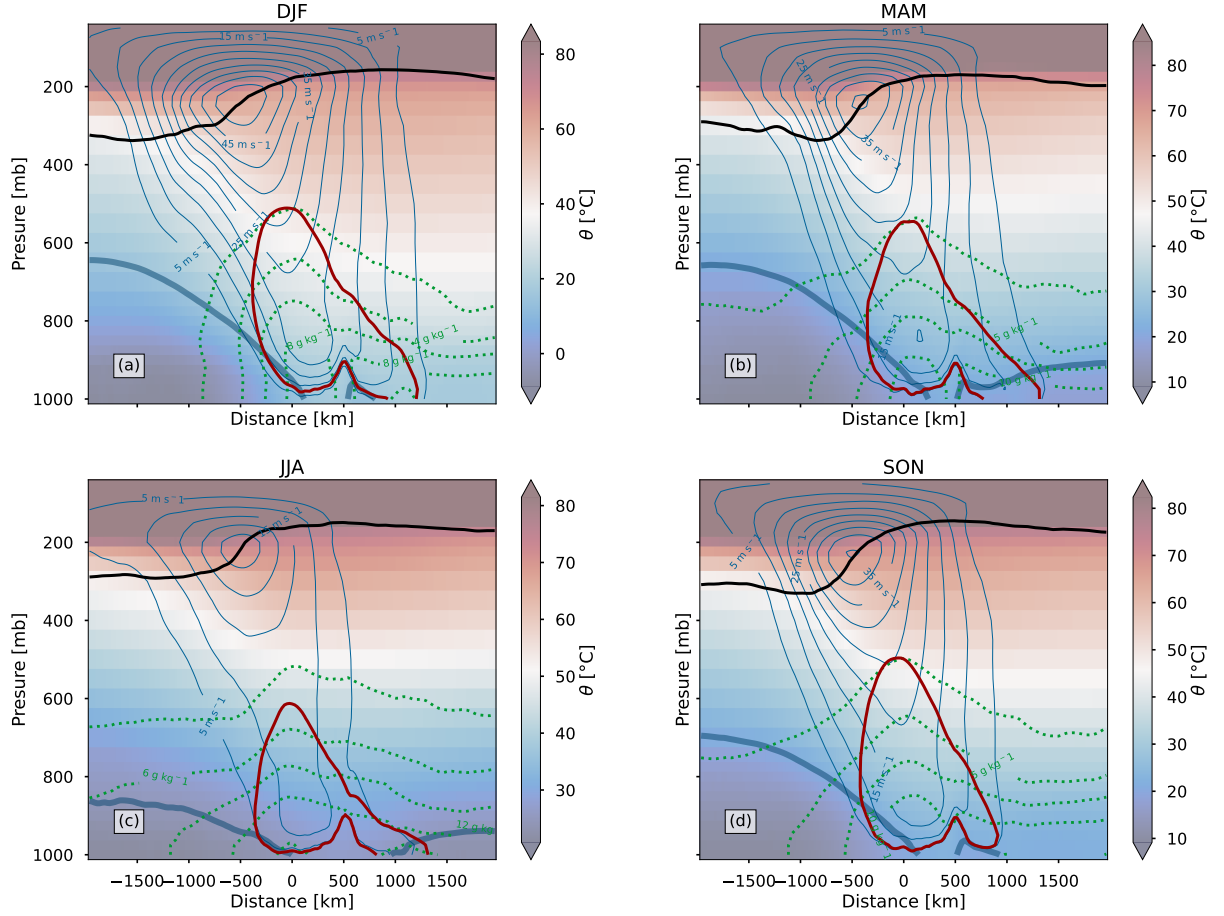


Figure 3. Composite transects of potential temperature (shading), transect-normal winds (blue curves), specific humidity (dotted green curves), moisture flux at the $60 \text{ g m kg}^{-1} \text{ s}^{-1}$ level (red contour), and the 2 PVU potential vorticity contour (black curve) for AR conditions over Bloomington, IN in (a) DJF, (b) MAM, (c) JJA, and (d) SON. Thick, transparent blue curves in all four panels show frontal zones. The trace of the transect is shown in Figure 2d.

region of high water vapor transport has a westward tilt, similar to the tilt in the tropospheric wind maximum, suggesting the importance of the upper level flow in generating the high IVT that defines the AR.

4 Discussion

Figures 1 and 3 bear a strong similarity to the map and transect plots shown by Ralph et al. (2018) in the American Meteorological Society Glossary definition of atmospheric rivers: strong, filamentary moisture transport to the southeast of a surface low and cold frontal zone; and high moisture transport associated with high surface humidity and southwesterly winds from an upper-level jet and a pre-frontal low-level jet. Based on the qualitative definition given by Ralph et al. (2018), and based on the objective detection of AR conditions by TECA-BARD, it seems clear that the ARs discussed here are phenomenologically similar to their western coastal counterparts.

Likewise, Figures 2 and 3 show the distinctive characteristics of a longwave baroclinic Rossby wave: an upper-level jet, presence of a frontal zone and a surface low, and

westward tilting wind and potential temperature fields indicative of baroclinic waves. The westward tilt in the moisture flux suggests that the moisture flux is associated with the synoptic-scale, geostrophically-driven winds. *This argues strongly against the hypothesis that central US atmospheric rivers are simply manifestations of the Great Plains low-level jet* (GPLLJ). The clear signature of a baroclinic wave and upper-level dynamics (e.g., the tropopause folds in Figure 3) indicate that the moisture flux is associated with synoptic processes rather than the more mesoscale (and possibly boundary layer) scale processes associated with the Great Plains low-level jet. Note that this does not rule out the possibility that the GPLLJ is present during these AR conditions; indeed, a masters thesis by Gyawali (2022) shows that most central Great Plains ARs also occur with a detected GPLLJ. But two factors suggest that synoptic-scale processes, rather than the GPLLJ, are the primary driver: (1) the similarity of the composites between seasons when the GPLLJ is not considered to be important (DJF) and seasons when it does have some influence (MAM and SON), and (2) Gyawali (2022) notes the similarity between mid-level height composites of AR+GPLLJ conditions and the dynamically-coupled GPLLJ composite conditions discussed by Burrows et al. (2019) in which the GPLLJ seems to be synoptically controlled.

Composites from all four seasons support the general idea that eastern US ARs are driven by longwave baroclinic Rossby waves, though there are some differences that are worth further investigation. The low amplitude of the upper-level wave in JJA (Figure 2c) may simply be related to the relatively weak meridional temperature gradient present at that time of year, or it may indicate that the composites are averages over multiple types of synoptic states such that the composite-mean pattern is weak. Additionally, DJF stands out from the other seasons in that the mean surface low is nearly co-located with the center of the AR (see Figure 2a) instead of being located well to the northwest of the AR. It is possible that surface convergence associated with lows in DJF may enable moisture—and resultant upper-level heating—from the AR to contribute to rapid deepening of these lows (Zhu & Newell, 1994; Z. Zhang et al., 2019). The use of simulation-based experiments and lagged composites may help clarify this.

There are two forms of uncertainty that may impact the conclusions here: uncertainty in the detection of ARs, and uncertainty associated with the choice of region over which to composite. Sensitivity tests using a different AR detection tool (from Guan and Waliser (2015)) and focus on a different region (Washington, DC) show qualitatively identical results: Figures S2–S5 for the ARDT sensitivity test; and Figures S3–S9 for the region sensitivity test. This suggests that the results presented here are robust to these sources of uncertainty.

Taken together, Figures 1–3 provide strong evidence that eastern US ARs are dynamically similar to their well-studied western US counterparts, though a key difference between the two is the mechanism for uplift and generation of precipitation. Orographic ascent in neutrally-stratified atmosphere provides an efficient mechanism for upward moisture flux (Neiman et al., 2002; Ralph et al., 2005; Neiman, Ralph, Wick, Kuo, et al., 2008; Cobb et al., 2021). The ubiquitous mountain ranges in the western US (e.g., the Coast Ranges, the Cascades, and the Sierra Nevadas) can provide this orographic forcing for ARs (B. L. Smith et al., 2010), though atmospheric stability and AR angle modulate the effectiveness of this orographic forcing (Neiman et al., 2002; Kingsmill et al., 2013; Hughes et al., 2014). In contrast, the relative dearth of topography in the area between the Rocky Mountains and the Appalachian mountains means that any upward moisture flux must come from dynamical and/or convective processes, such as isentropic lift or convective instability.

Analysis of composite vertical velocities shows a broad area of low-level updraft across the majority of the AR region: Figure 4 shows composite vertical velocities at 700 hPa (in pressure coordinates: negative velocities indicate upward motion) over regions where IVT is greater than the $250 \text{ kg m}^{-1} \text{ s}^{-1}$ threshold that is often used as a baseline for AR

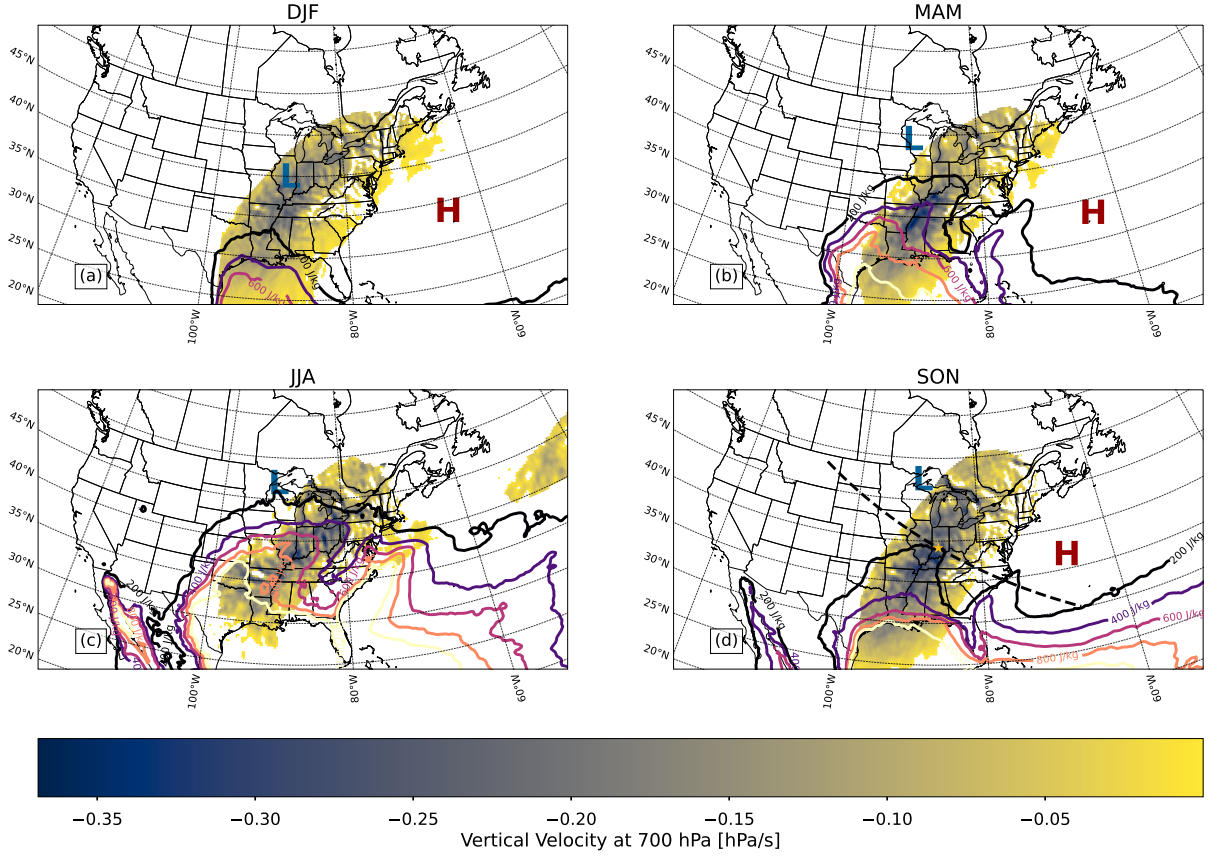


Figure 4. Composite of upward vertical velocity at 700 mb within regions of IVT higher than $250 \text{ kg m}^{-1} \text{ s}^{-1}$, CAPE (colored contours), and the location of lows, highs, and the transect trace as in Figure 2.

presence (Rutz et al., 2014). These velocities reach up to -0.3 hPa s^{-1} in all seasons. Considering that Figure 3 shows specific humidity values in the range $1\text{--}10 \text{ g kg}^{-1}$, this corresponds to a vertical moisture flux of $\mathcal{O}(0.1) \text{ mm d}^{-1}$ or smaller. A moisture flux of this magnitude is too low to explain the extreme precipitation associated with AR conditions as discussed by Slinsky et al. (2020) and shown in Figure S1. However, this broad region of synoptic-scale uplift may be enough to initiate convection.

Among the four seasons, all but DJF have appreciable mean convectively available potential energy (CAPE; see Figure 4 and Figures S5, S9) over the study region, and even DJF shows hints of elevated CAPE extending from the Gulf of Mexico. This suggests that ARs in this region fuel convection through providing: (1) an adequate supply of high moisture content, (2) a source of unstable air, and (3) a broad region of upward motion. Even absent an orographic source of uplift, these three factors combine to provide an efficient mechanism for translating horizontal moisture flux into intense vertical moisture flux within convective regions. These three ingredients, in combination with the wind shear (Figure 2) associated with the growing baroclinic wave that drives the AR, are well-known ingredients for severe convective environments. One therefore might expect a strong association between mesoscale convective systems (MCS) and ARs in this region, and this warrants further study.

This association between ARs and environments favorable for MCS development may also open new opportunities for using paleoclimate proxies to study ARs and cli-

mate change. For the western US, the presence of terrigenous sediment layers can provide a proxy of AR-driven activity, since terrestrial flood events tend to be primarily associated with ARs in the region (Hendy et al., 2015; Du et al., 2018). Such a proxy is inapplicable in the continental interior, but recent work by Sun et al. (2021) shows that the hydrogen isotopic composition of leaf wax preserves a signal associated with MCS. The authors primarily associate this proxy with changes in the GPLLJ, but analysis of paleoclimate simulations suggest that ARs—and changes therein—may have played a major factor in the hydroclimate of the continental interior since the Last Glacial Maximum (Skinner et al., 2020; Lora et al., 2023; Skinner et al., 2023). Taken together, the analysis here suggests that ARs may be a factor in modulating MCS activity in the region. Further analysis of the proxy developed by Sun et al. (2021) may provide a novel way to study paleoclimate changes in ARs in the continental interior.

5 Conclusions

This analysis provides clear evidence that ARs in the eastern US are driven by synoptic-scale processes, and in particular that ARs seem to be associated with longwave baroclinic Rossby waves. This does not preclude the idea that the GPLLJ can sometimes play a role in these ARs, but the evidence presented here suggests that the primary means of generating strong, and southwesterly, horizontal moisture flux is through geostrophic forcing of winds from a synoptic-scale wave. This horizontal moisture flux—and associated unstable air—then drives vertical moisture flux (and precipitation) through convective processes rather than orographic processes as in the western US.

As Slinskey et al. (2020) report, a high proportion of central and eastern US extreme precipitation is associated with ARs, but it is not known whether this extreme precipitation results from ARs alone. Figure S1 indicates that some extreme precipitation events are associated with more than one meteorological phenomenon (e.g., a front, an AR, and a mesoscale convective system as in that case), and analysis of Figures 2, 3, and 4 suggest that these ARs occur in an environment favorable for mesoscale convection. It is not clear how frequently such co-occurrences happen or whether they systematically intensify precipitation. We are currently working on follow-up studies to assess this.

Given that eastern US ARs are synoptically forced, it seems reasonable to expect that climate models should be able to resolve this association between midlatitude cyclones and ARs in this region. Indeed, a recent intercomparison of simulations and AR detection tools shows that most climate models simulate a relative maximum in AR frequency in the midwestern and eastern US (O’Brien et al., 2021), suggesting that this may be the case. Building composites, like the ones shown here but for historical climate model simulations, could provide a way to directly evaluate the dynamics of simulated ARs. In contrast, the mechanisms for vertical moisture flux—which appear to be convective in nature—could be quite challenging for models to adequately simulate. Such a phenomenon-focused perspective could provide a way to elucidate specific model deficiencies as well as possible indications for how to fix them. A recent workshop has advocated for such an approach as a promising way to rapidly improve the simulation of precipitation in climate models (Pendergrass et al., 2020).

This work helps pave the way for advancing a theory-based understanding of ARs and climate change in the eastern US that builds on the well-established thermodynamic scaling of moisture (i.e., Clauius-Clapeyron scaling) in ARs (Payne et al., 2020). The results here show that eastern US ARs are strongly associated with midlatitude cyclones, and there is an increasing body of literature about the theoretical effects of climate change on the location and frequency of these storms (Shaw et al., 2016; Feldl et al., 2017; Shaw, 2019). Overall, it could be beneficial to extend this work further to assess the degree to which different areas of high AR frequency—particularly the inland ones—seem to be associated with midlatitude cyclones.

Open Research Section

The European Centre for Medium-Range Weather Forecasts ERA5 Reanalysis (0.25 Degree Latitude-Longitude Grid) dataset was provided by the Research Data Archive at the National Center for Atmospheric Research, Computational and Information Systems Laboratory. <https://doi.org/10.5065/BH6N-5N20>

Atmospheric river detections from `teca_bard_v1.0.1` and `guan_waliser_v2` are available as part of the Atmospheric River Tracking Method Intercomparison Project Tier 1 experiment archive. <https://doi.org/10.5065/D6R78D1M>

Acknowledgments

This material is based upon work supported by the U.S. Department of Energy, Office of Science, Office of Biological and Environmental Research, Climate and Environmental Sciences Division, Regional & Global Model Analysis Program and used resources of the National Energy Research Scientific Computing Center (NERSC), also supported by the Office of Science of the U.S. Department of Energy under Contract No. DE-AC02-05CH11231. This research was also supported in part by the Environmental Resilience Institute, funded by Indiana University's Prepared for Environmental Change Grand Challenge initiative and in part by Lilly Endowment, Inc., through its support for the Indiana University Pervasive Technology Institute.

TAO designed the study, performed the data analysis, and wrote the original draft of the paper. BL, AD, and TAO contributed software (the Toolkit for Extreme Climate Analysis) central to the study. MRI, DK, KQ, and CK contributed to interpretation of the results and the writing of the original draft. All authors contributed to the review and editing of the final manuscript.

References

- Bao, J. W., Michelson, S. A., Neiman, P. J., Ralph, F. M., & Wilczak, J. M. (2006). Interpretation of enhanced integrated water vapor bands associated with extratropical cyclones: Their formation and connection to tropical moisture. *Monthly Weather Review*, *134*(4), 1063–1080. doi: 10.1175/MWR3123.1
- Burrows, D. A., Ferguson, C. R., Campbell, M. A., Xia, G., & Bosart, L. F. (2019, nov). An Objective Classification and Analysis of Upper-Level Coupling to the Great Plains Low-Level Jet over the Twentieth Century. *Journal of Climate*, *32*(21), 7127–7152. Retrieved from <http://journals.ametsoc.org/doi/10.1175/JCLI-D-18-0891.1> doi: 10.1175/JCLI-D-18-0891.1
- Cao, Q., Gershunov, A., Shulgina, T., Ralph, F. M., Sun, N., & Lettenmaier, D. P. (2020, aug). Floods due to Atmospheric Rivers along the U.S. West Coast: The Role of Antecedent Soil Moisture in a Warming Climate. *Journal of Hydrometeorology*, *21*(8), 1827–1845. Retrieved from <https://journals.ametsoc.org/view/journals/hydr/21/8/jhmD190242.xml> doi: 10.1175/JHM-D-19-0242.1
- Cao, Q., Shukla, S., DeFlorio, M. J., Ralph, F. M., & Lettenmaier, D. P. (2021, apr). Evaluation of the subseasonal forecast skill of floods associated with atmospheric rivers in coastal Western U.S. watersheds. *Journal of Hydrometeorology*, *22*(6), 1535–1552. Retrieved from <https://journals.ametsoc.org/view/journals/hydr/aop/JHM-D-20-0219.1/JHM-D-20-0219.1.xml> doi: 10.1175/JHM-D-20-0219.1
- Cobb, A., Michaelis, A., Iacobellis, S., Ralph, F. M., & Delle Monache, L. (2021, mar). Atmospheric River Sectors: Definition and Characteristics Observed Using Dropsondes from 2014–20 CalWater and AR Recon. *Monthly Weather Review*, *149*(3), 623–644. Retrieved from <https://journals.ametsoc.org/>

- view/journals/mwre/aop/MWR-D-20-0177.1/MWR-D-20-0177.1.xmlhttps://
journals.ametsoc.org/view/journals/mwre/149/3/MWR-D-20-0177.1.xml
doi: 10.1175/MWR-D-20-0177.1
- Collow, A. B. M., Shields, C. A., Guan, B., Kim, S., Lora, J. M., McClenny, E. E.,
... Wehner, M. (2022, apr). An Overview of ARTMIP's Tier 2 Reanalysis In-
tercomparison: Uncertainty in the Detection of Atmospheric Rivers and Their
Associated Precipitation. *Journal of Geophysical Research: Atmospheres*,
127(8). Retrieved from https://onlinelibrary.wiley.com/doi/10.1029/
2021JD036155 doi: 10.1029/2021JD036155
- Cordeira, J. M., Martin Ralph, F., & Moore, B. J. (2013). The development and
evolution of two atmospheric rivers in proximity to western north pacific trop-
ical cyclones in october 2010. *Monthly Weather Review*, 141(12), 4234–4255.
doi: 10.1175/MWR-D-13-00019.1
- Dacre, H. F., Clark, P. A., Martinez-Alvarado, O., Stringer, M. A., & Lavers, D. A.
(2015). How do atmospheric rivers form? *Bulletin of the American Meteorolog-
ical Society*, 96(8), 1243–1255. doi: 10.1175/BAMS-D-14-00031.1
- DeFlorio, M. J., Waliser, D. E., Guan, B., Lavers, D. A., Ralph, F. M., & Vi-
tart, F. (2018, feb). Global Assessment of Atmospheric River Predic-
tion Skill. *Journal of Hydrometeorology*, 19(2), 409–426. Retrieved from
http://journals.ametsoc.org/doi/10.1175/JHM-D-17-0135.1 doi:
10.1175/JHM-D-17-0135.1
- DeFlorio, M. J., Waliser, D. E., Guan, B., Ralph, F. M., & Vitart, F. (2019, mar).
Global evaluation of atmospheric river subseasonal prediction skill. *Cli-
mate Dynamics*, 52(5-6), 3039–3060. Retrieved from https://doi.org/
10.1007/s00382-018-4309-x.http://link.springer.com/10.1007/
s00382-018-4309-x doi: 10.1007/s00382-018-4309-x
- Dettinger, M. (2011). Climate change, atmospheric rivers, and floods in Cali-
fornia - a multimodel analysis of storm frequency and magnitude changes.
Journal of the American Water Resources Association, 47(3), 514–523. doi:
10.1111/j.1752-1688.2011.00546.x
- Dirmeyer, P. A., & Kinter, J. L. (2009). The "Maya Express": Floods in the U.S.
Midwest. *Eos*, 90(12), 101–102. doi: 10.1029/2009EO120001
- Dirmeyer, P. A., & Kinter, J. L. (2010). Floods over the U.S. midwest: A regional
water cycle perspective. *Journal of Hydrometeorology*, 11(5), 1172–1181. doi:
10.1175/2010JHM1196.1
- Dong, L., Leung, L. R., Song, F., & Lu, J. (2018). Roles of SST versus internal
atmospheric variability in winter extreme precipitation variability along the
U.S. West Coast. *Journal of Climate*, JCLI-D-18-0062.1. Retrieved from
http://journals.ametsoc.org/doi/10.1175/JCLI-D-18-0062.1 doi:
10.1175/JCLI-D-18-0062.1
- Du, X., Hendy, I., & Schimmelmanna, A. (2018). A 9000-year flood history
for Southern California: A revised stratigraphy of varved sediments in
Santa Barbara Basin. *Marine Geology*, 397(November 2017), 29–42. Re-
trieved from https://doi.org/10.1016/j.margeo.2017.11.014 doi:
10.1016/j.margeo.2017.11.014
- Eiras-Barca, J., Ramos, A. M., Pinto, J. G., Trigo, R. M., Liberato, M. L. R., &
Miguez-Macho, G. (2018, jan). The concurrence of atmospheric rivers and ex-
plosive cyclogenesis in the North Atlantic and North Pacific basins. *Earth Sys-
tem Dynamics*, 9(1), 91–102. Retrieved from https://esd.copernicus.org/
articles/9/91/2018/ doi: 10.5194/esd-9-91-2018
- Espinoza, V., Waliser, D. E., Guan, B., Lavers, D. A., & Ralph, F. M. (2018, may).
Global Analysis of Climate Change Projection Effects on Atmospheric Rivers.
Geophysical Research Letters, 45(9), 4299–4308. Retrieved from http://
doi.wiley.com/10.1029/2017GL076968 doi: 10.1029/2017GL076968
- European Centre for Medium-Range Weather Forecasts. (2019). *Era5 reanalysis*

- (0.25 degree latitude-longitude grid). Boulder CO: Research Data Archive at the National Center for Atmospheric Research, Computational and Information Systems Laboratory. Retrieved from <https://doi.org/10.5065/BH6N-5N20>
- Feldl, N., Anderson, B. T., & Bordoni, S. (2017). Atmospheric eddies mediate lapse rate feedback and arctic amplification. *Journal of Climate*, 30(22), 9213–9224. doi: 10.1175/JCLI-D-16-0706.1
- Feng, Z., Leung, L. R., Houze, R. A., Hagos, S., Hardin, J., Yang, Q., ... Fan, J. (2018, jul). Structure and Evolution of Mesoscale Convective Systems: Sensitivity to Cloud Microphysics in Convection-Permitting Simulations Over the United States. *Journal of Advances in Modeling Earth Systems*, 10(7), 1470–1494. Retrieved from <https://onlinelibrary.wiley.com/doi/10.1029/2018MS001305> doi: 10.1029/2018MS001305
- Gao, Y., Lu, J., Leung, L. R., Yang, Q., Hagos, S., & Qian, Y. (2015, sep). Dynamical and thermodynamical modulations on future changes of landfalling atmospheric rivers over western North America. *Geophysical Research Letters*, 42(17), 7179–7186. Retrieved from <http://doi.wiley.com/10.1002/2015GL065435> doi: 10.1002/2015GL065435
- Gebauer, J. G., & Shapiro, A. (2019). Clarifying the baroclinic contribution to the great plains low-level jet frequency maximum. *Monthly Weather Review*, 147(9), 3481–3493. doi: 10.1175/MWR-D-19-0024.1
- Gelaro, R., McCarty, W., Suárez, M. J., Todling, R., Molod, A., Takacs, L., ... Zhao, B. (2017, jul). The Modern-Era Retrospective Analysis for Research and Applications, Version 2 (MERRA-2). *Journal of Climate*, 30(14), 5419–5454. Retrieved from <http://journals.ametsoc.org/doi/10.1175/JCLI-D-16-0758.1> doi: 10.1175/JCLI-D-16-0758.1
- Gershunov, A., Shulgina, T., Ralph, F. M., Lavers, D. A., & Rutz, J. J. (2017, aug). Assessing the climate-scale variability of atmospheric rivers affecting western North America. *Geophysical Research Letters*, 44(15), 7900–7908. Retrieved from <http://doi.wiley.com/10.1002/2017GL074175> doi: 10.1002/2017GL074175
- Gimeno, L., Dominguez, F., Nieto, R., Trigo, R., Drumond, A., Reason, C. J., ... Marengo, J. (2016). Major Mechanisms of Atmospheric Moisture Transport and Their Role in Extreme Precipitation Events. *Annual Review of Environment and Resources*, 41(1), 117–141. doi: 10.1146/annurev-environ-110615-085558
- Gimeno, L., Drumond, A., Nieto, R., Trigo, R. M., & Stohl, A. (2010). On the origin of continental precipitation. *Geophysical Research Letters*, 37(13). Retrieved from <https://agupubs.onlinelibrary.wiley.com/doi/abs/10.1029/2010GL043712> doi: <https://doi.org/10.1029/2010GL043712>
- Gorodetskaya, I. V., Tsukernik, M., Claes, K., Ralph, M. F., Neff, W. D., & Van Lipzig, N. P. M. (2014, sep). The role of atmospheric rivers in anomalous snow accumulation in East Antarctica. *Geophysical Research Letters*, 41(17), 6199–6206. Retrieved from <http://doi.wiley.com/10.1002/2014GL060881> doi: 10.1002/2014GL060881
- Griffith, H. V., Wade, A. J., Lavers, D. A., & Watts, G. (2020). Atmospheric river orientation determines flood occurrence. *Hydrological Processes*(September), 4547–4555. doi: 10.1002/hyp.13905
- Guan, B., & Waliser, D. E. (2015, dec). Detection of atmospheric rivers: Evaluation and application of an algorithm for global studies. *Journal of Geophysical Research: Atmospheres*, 120(24), 12514–12535. Retrieved from <http://doi.wiley.com/10.1002/2015JD024257> doi: 10.1002/2015JD024257
- Guan, B., Waliser, D. E., Molotch, N. P., Fetzner, E. J., & Neiman, P. J. (2011). Does the Madden–Julian Oscillation Influence Wintertime Atmospheric Rivers and Snowpack in the Sierra Nevada? *Monthly Weather Review*, 140(2), 325–

342. doi: 10.1175/mwr-d-11-00087.1
- Guo, Y., Shinoda, T., Guan, B., Waliser, D. E., & Chang, E. K. (2020). Statistical relationship between atmospheric rivers and extratropical cyclones and anticyclones. *Journal of Climate*, 33(18), 7817–7834. doi: 10.1175/JCLI-D-19-0126.1
- Gyawali, N. (2022). *A Comparative Analysis of the Impact of Low-Level Jets and Atmospheric Rivers in the Central U.S* (Doctoral dissertation, State University of New York at Albany). Retrieved from <https://proxyiub.uits.iu.edu/login?url=https%3A%2F%2Fwww.proquest.com%2Fdissertations-theses%2Fcomparative-analysis-impact-low-level-jets%2Fdocview%2F2708702323%2Fse-2%3Faccountid%3D11620>
- Hagos, S. M., Leung, L. R., Yoon, J.-h., Lu, J., & Gao, Y. (2016, feb). A projection of changes in landfalling atmospheric river frequency and extreme precipitation over western North America from the Large Ensemble CESM simulations. *Geophysical Research Letters*, 43(3), 1357–1363. Retrieved from <https://onlinelibrary.wiley.com/doi/10.1002/2015GL067392> doi: 10.1002/2015GL067392
- Hendy, I. L., Napier, T. J., & Schimmelmann, A. (2015, nov). From extreme rainfall to drought: 250 years of annually resolved sediment deposition in Santa Barbara Basin, California. *Quaternary International*, 387, 3–12. Retrieved from <http://dx.doi.org/10.1016/j.quaint.2015.01.026><https://linkinghub.elsevier.com/retrieve/pii/S104061821500049X> doi: 10.1016/j.quaint.2015.01.026
- Hersbach, H., Bell, B., Berrisford, P., Hirahara, S., Horányi, A., Muñoz-Sabater, J., ... Thépaut, J. (2020, jul). The ERA5 global reanalysis. *Quarterly Journal of the Royal Meteorological Society*, 146(730), 1999–2049. Retrieved from <https://onlinelibrary.wiley.com/doi/10.1002/qj.3803> doi: 10.1002/qj.3803
- Holton, J. (2004). *An introduction to dynamic meteorology*. Elsevier Science. Retrieved from <https://books.google.com/books?id=fhW5oDv3EPsC>
- Hughes, M., Mahoney, K. M., Neiman, P. J., Moore, B. J., Alexander, M., & Ralph, F. M. (2014). The landfall and inland penetration of a flood-producing atmospheric river in Arizona. Part II: Sensitivity of modeled precipitation to terrain height and atmospheric river orientation. *Journal of Hydrometeorology*, 15(5), 1954–1974. doi: 10.1175/JHM-D-13-0176.1
- Kingsmill, D. E., Neiman, P. J., Moore, B. J., Hughes, M., Yuter, S. E., & Ralph, F. M. (2013, jun). Kinematic and Thermodynamic Structures of Sierra Barrier Jets and Overrunning Atmospheric Rivers during a Landfalling Winter Storm in Northern California. *Monthly Weather Review*, 141(6), 2015–2036. Retrieved from <https://journals.ametsoc.org/view/journals/mwre/141/6/mwr-d-12-00277.1.xml> doi: 10.1175/MWR-D-12-00277.1
- Knippertz, P., & Wernli, H. (2010). A lagrangian climatology of tropical moisture exports to the northern hemispheric extratropics. *Journal of Climate*, 23(4), 987–1003. doi: 10.1175/2009JCLI3333.1
- Lavers, D. A., Pappenberger, F., Richardson, D. S., & Zsoter, E. (2016). ECMWF Extreme Forecast Index for water vapor transport: A forecast tool for atmospheric rivers and extreme precipitation. *Geophysical Research Letters*, 43(22), 11,852–11,858. doi: 10.1002/2016GL071320
- Lavers, D. A., Ralph, F. M., Richardson, D. S., & Pappenberger, F. (2020, dec). Improved forecasts of atmospheric rivers through systematic reconnaissance, better modelling, and insights on conversion of rain to flooding. *Communications Earth & Environment*, 1(1), 39. Retrieved from <http://dx.doi.org/10.1038/s43247-020-00042-1><http://www.nature.com/articles/s43247-020-00042-1> doi: 10.1038/s43247-020-00042-1
- Lavers, D. A., & Villarini, G. (2013, oct). Atmospheric Rivers and Flooding over

- the Central United States. *Journal of Climate*, 26(20), 7829–7836. Retrieved from <http://journals.ametsoc.org/doi/10.1175/JCLI-D-13-00212.1> doi: 10.1175/JCLI-D-13-00212.1
- Lavers, D. A., Villarini, G., Allan, R. P., Wood, E. F., & Wade, A. J. (2012, oct). The detection of atmospheric rivers in atmospheric reanalyses and their links to British winter floods and the large-scale climatic circulation. *Journal of Geophysical Research Atmospheres*, 117(20), 1–13. Retrieved from <http://doi.wiley.com/10.1029/2012JD018027> doi: 10.1029/2012JD018027
- Lavers, D. A., Waliser, D. E., Ralph, F. M., & Dettinger, M. D. (2016). Predictability of horizontal water vapor transport relative to precipitation: Enhancing situational awareness for forecasting western U.S. extreme precipitation and flooding. *Geophysical Research Letters*, 43(5), 2275–2282. doi: 10.1002/2016GL067765
- Leung, L.-R., & Qian, Y. (2009). Atmospheric rivers induced heavy precipitation and flooding in the western U.S. simulated by the WRF regional climate model. *Geophysical Research Letters*, 36(3), 1–6. doi: 10.1029/2008GL036445
- Liang, P., Dong, G., Zhang, H., Zhao, M., & Ma, Y. (2020). Atmospheric rivers associated with summer heavy rainfall over the Yangtze Plain. *Journal of Southern Hemisphere Earth Systems Science*. doi: 10.1071/es19028
- Lora, J. M., Mitchell, J. L., Risi, C., & Tripathi, A. E. (2017, jan). North Pacific atmospheric rivers and their influence on western North America at the Last Glacial Maximum. *Geophysical Research Letters*, 44(2), 1051–1059. Retrieved from <http://doi.wiley.com/10.1002/2016GL071541> <https://onlinelibrary.wiley.com/doi/abs/10.1002/2016GL071541> doi: 10.1002/2016GL071541
- Lora, J. M., Shields, C. A., & Rutz, J. J. (2020, oct). Consensus and Disagreement in Atmospheric River Detection: ARTMIP Global Catalogues. *Geophysical Research Letters*, 47(20), 1–10. Retrieved from <https://onlinelibrary.wiley.com/doi/10.1029/2020GL089302> doi: 10.1029/2020GL089302
- Lora, J. M., Skinner, C. B., Rush, W. D., & Baek, S. H. (2023). The Hydrologic Cycle and Atmospheric Rivers in CESM2 Simulations of the Last Glacial Maximum. *Geophysical Research Letters*, 50(18), 1–11. doi: 10.1029/2023GL104805
- Loring, B., Elbashandy, A., O'Brien, T. A., HarinarayanKrishnan, amandasd, & noel. (2022, June). *Lbl-eesa/teca: Teca 5.0.0*. Zenodo. Retrieved from <https://doi.org/10.5281/zenodo.6640288> doi: 10.5281/zenodo.6640288
- Ma, W., & Chen, G. (2022, aug). What Controls the Interannual Variability of the Boreal Winter Atmospheric River Activities over the Northern Hemisphere? *Journal of Climate*, 1–39. Retrieved from <https://journals.ametsoc.org/view/journals/clim/aop/JCLI-D-22-0089.1/JCLI-D-22-0089.1.xml> doi: 10.1175/JCLI-D-22-0089.1
- Mahoney, K. M., Jackson, D. L., Neiman, P., Hughes, M., Darby, L., Wick, G., ... Cifelli, R. (2016). Understanding the role of atmospheric rivers in heavy precipitation in the southeast United States. *Monthly Weather Review*, 144(4), 1617–1632. doi: 10.1175/MWR-D-15-0279.1
- Massoud, E., Massoud, T., Guan, B., Sengupta, A., Espinoza, V., De Luna, M. D., ... Waliser, D. (2020). Atmospheric Rivers and Precipitation in the Middle East and North Africa (MENA). *Water*, 12(10), 2863. doi: 10.3390/w12102863
- McClenny, E. E., Ullrich, P. A., & Grotjahn, R. (2020, nov). Sensitivity of Atmospheric River Vapor Transport and Precipitation to Uniform Sea Surface Temperature Increases. *Journal of Geophysical Research: Atmospheres*, 125(21), 1–20. Retrieved from <https://onlinelibrary.wiley.com/doi/10.1029/2020JD033421> doi: 10.1029/2020JD033421
- Moore, B. J., Neiman, P. J., Ralph, F. M., & Barthold, F. E. (2012). Physi-

- cal processes associated with heavy flooding rainfall in nashville, tennessee, and vicinity during 1-2 may 2010: The role of an atmospheric river and mesoscale convective systems. *Monthly Weather Review*, 140(2), 358–378. doi: 10.1175/MWR-D-11-00126.1
- Mundhenk, B. D., Barnes, E. A., & Maloney, E. D. (2016). All-season climatology and variability of atmospheric river frequencies over the North Pacific. *Journal of Climate*, 29(13), 4885–4903. doi: 10.1175/JCLI-D-15-0655.1
- Mundhenk, B. D., Barnes, E. A., Maloney, E. D., & Baggett, C. F. (2018, dec). Skillful empirical subseasonal prediction of landfalling atmospheric river activity using the Madden–Julian oscillation and quasi-biennial oscillation. *npj Climate and Atmospheric Science*, 1(1), 20177. Retrieved from <http://dx.doi.org/10.1038/s41612-017-0008-2> <http://www.nature.com/articles/s41612-017-0008-2> doi: 10.1038/s41612-017-0008-2
- Nakamura, J., Lall, U., Kushnir, Y., Robertson, A. W., & Seager, R. (2013). Dynamical structure of extreme floods in the U.S. Midwest and the United Kingdom. *Journal of Hydrometeorology*, 14(2), 485–504. doi: 10.1175/JHM-D-12-059.1
- Nash, D., Carvalho, L. M. V., Jones, C., & Ding, Q. (2021, oct). Winter and spring atmospheric rivers in High Mountain Asia: climatology, dynamics, and variability. *Climate Dynamics*(0123456789). Retrieved from <https://doi.org/10.1007/s00382-021-06008-z> <https://link.springer.com/10.1007/s00382-021-06008-z> doi: 10.1007/s00382-021-06008-z
- Nash, D., Waliser, D., Guan, B., Ye, H., & Ralph, F. M. (2018, jul). The Role of Atmospheric Rivers in Extratropical and Polar Hydroclimate. *Journal of Geophysical Research: Atmospheres*, 123(13), 6804–6821. Retrieved from <https://doi.org/10.1029/2017JD028130> <https://onlinelibrary.wiley.com/doi/abs/10.1029/2017JD028130> doi: 10.1029/2017JD028130
- Nayak, M. A., Villarini, G., & Allen Bradley, A. (2016). Atmospheric rivers and rainfall during NASA’s Iowa Flood Studies (IFloodS) campaign. *Journal of Hydrometeorology*, 17(1), 257–271. doi: 10.1175/JHM-D-14-0185.1
- Neiman, P. J., Ralph, F. M., White, A. B., Kingsmill, D. E., & Persson, P. O. (2002). The statistical relationship between upslope flow and rainfall in California’s coastal mountains: Observations during CALJET. *Monthly Weather Review*, 130(6), 1468–1492. doi: 10.1175/1520-0493(2002)130<1468:TSRBUF>2.0.CO;2
- Neiman, P. J., Ralph, F. M., Wick, G. A., Kuo, Y. H., Wee, T. K., Ma, Z., ... Dettinger, M. D. (2008). Diagnosis of an intense atmospheric river impacting the pacific northwest: Storm summary and offshore vertical structure observed with COSMIC satellite retrievals. *Monthly Weather Review*, 136(11), 4398–4420. doi: 10.1175/2008MWR2550.1
- Neiman, P. J., Ralph, F. M., Wick, G. A., Lundquist, J. D., & Dettinger, M. D. (2008). Meteorological characteristics and overland precipitation impacts of atmospheric rivers affecting the West coast of North America based on eight years of SSM/I satellite observations. *Journal of Hydrometeorology*, 9(1), 22–47. doi: 10.1175/2007JHM855.1
- Newell, R. E., Newell, N. E., Zhu, Y., & Scott, C. (1992, dec). Tropospheric rivers? - A pilot study. *Geophysical Research Letters*, 19(24), 2401–2404. Retrieved from <http://doi.wiley.com/10.1029/92GL02916> doi: 10.1029/92GL02916
- Newell, R. E., & Zhu, Y. (1994, jan). Tropospheric rivers: A one-year record and a possible application to ice core data. *Geophysical Research Letters*, 21(2), 113–116. Retrieved from <http://doi.wiley.com/10.1029/93GL03113> doi: 10.1029/93GL03113
- Newman, M., Kiladis, G. N., Weickmann, K. M., Ralph, M. F., & Sardeshmukh, P. D. (2012). Relative contributions of synoptic and low-frequency eddies to time-mean atmospheric moisture transport, including the role of at-

- mospheric rivers. *Journal of Climate*, 25(21), 7341–7361. doi: 10.1175/JCLI-D-11-00665.1
- O'Brien, T. A., Risser, M. D., Loring, B., Elbashandy, A. A., Krishnan, H., Johnson, J., ... Collins, W. D. (2020, dec). Detection of atmospheric rivers with inline uncertainty quantification: TECA-BARD v1.0.1. *Geoscientific Model Development*, 13(12), 6131–6148. Retrieved from <https://www.geosci-model-dev-discuss.net/gmd-2020-55/#discussion><https://gmd.copernicus.org/articles/13/6131/2020/> doi: 10.5194/gmd-13-6131-2020
- O'Brien, T. A., Wehner, M. F., Payne, A. E., Shields, C. A., Rutz, J. J., Leung, L., ... Zhou, Y. (2021, dec). Increases in Future AR Count and Size: Overview of the ARTMIP Tier 2 CMIP5/6 Experiment. *Journal of Geophysical Research: Atmospheres*, 24. Retrieved from <https://doi.org/10.1002/essoar.10504170.2><https://onlinelibrary.wiley.com/doi/10.1029/2021JD036013> doi: 10.1029/2021JD036013
- Payne, A. E., Demory, M.-E., Leung, L. R., Ramos, A. M., Shields, C. A., Rutz, J. J., ... Ralph, F. M. (2020, mar). Responses and impacts of atmospheric rivers to climate change. *Nature Reviews Earth & Environment*, 1(3), 143–157. Retrieved from <http://dx.doi.org/10.1038/s43017-020-0030-5><http://www.nature.com/articles/s43017-020-0030-5> doi: 10.1038/s43017-020-0030-5
- Payne, A. E., & Magnusdottir, G. (2015, nov). An evaluation of atmospheric rivers over the North Pacific in CMIP5 and their response to warming under RCP 8.5. *Journal of Geophysical Research: Atmospheres*, 120(21), 11,173–11,190. Retrieved from <http://doi.wiley.com/10.1002/2015JD023586> doi: 10.1002/2015JD023586
- Pendergrass, A. G., Gleckler, P. J., Leung, L. R., & Jakob, C. (2020, jun). Benchmarking Simulated Precipitation in Earth System Models. *Bulletin of the American Meteorological Society*, 101(6), E814–E816. Retrieved from <https://journals.ametsoc.org/view/journals/bams/101/6/bamsD190318.xml> doi: 10.1175/BAMS-D-19-0318.1
- Prabhat, Byna, S., Vishwanath, V., Dart, E., Wehner, M., & Collins, W. D. (2015). Teca: Petascale pattern recognition for climate science. In G. Azzopardi & N. Petkov (Eds.), *Computer analysis of images and patterns* (pp. 426–436). Cham: Springer International Publishing.
- Ralph, F. M., Coleman, T., Neiman, P. J., Zamora, R. J., & Dettinger, M. D. (2013, apr). Observed Impacts of Duration and Seasonality of Atmospheric-River Landfalls on Soil Moisture and Runoff in Coastal Northern California. *Journal of Hydrometeorology*, 14(2), 443–459. Retrieved from <https://journals.ametsoc.org/jhm/article/14/2/443/5819/Observed-Impacts-of-Duration-and-Seasonality-of> doi: 10.1175/JHM-D-12-076.1
- Ralph, F. M., & Dettinger, M. D. (2012). Historical and national perspectives on extreme west coast precipitation associated with atmospheric rivers during december 2010. *Bulletin of the American Meteorological Society*, 93(6), 783–790. doi: 10.1175/BAMS-D-11-00188.1
- Ralph, F. M., Dettinger, M. D., Cairns, M. M., Galarneau, T. J., & Eylander, J. (2018, apr). Defining “Atmospheric River”: How the Glossary of Meteorology Helped Resolve a Debate. *Bulletin of the American Meteorological Society*, 99(4), 837–839. Retrieved from <http://journals.ametsoc.org/doi/10.1175/BAMS-D-17-0157.1> doi: 10.1175/BAMS-D-17-0157.1
- Ralph, F. M., Neiman, P. J., & Rotunno, R. (2005). Dropsonde observations in low-level jets over the northeastern Pacific Ocean from CALJET-1998 and PACJET-2001: Mean vertical-profile and atmospheric-river characteristics. *Monthly Weather Review*, 133(4), 889–910. doi: 10.1175/MWR2896.1
- Ralph, F. M., Neiman, P. J., & Wick, G. A. (2004). Satellite and CALJET aircraft observations of atmospheric rivers over the Eastern North Pacific Ocean during

- the winter of 1997/98. *Monthly Weather Review*, 132(7), 1721–1745. doi: 10.1175/1520-0493(2004)132<1721:SACAOO>2.0.CO;2
- Ralph, F. M., Neiman, P. J., Wick, G. A., Gutman, S. I., Dettinger, M. D., Cayan, D. R., & White, A. B. (2006). Flooding on California’s Russian River: Role of atmospheric rivers. *Geophysical Research Letters*, 33(13), L13801. Retrieved from <https://doi.org/10.1029/2006GL026689>. <http://doi.wiley.com/10.1029/2006GL026689> doi: 10.1029/2006GL026689
- Ralph, F. M., Rutz, J. J., Cordeira, J. M., Dettinger, M., Anderson, M., Reynolds, D., ... Smallcomb, C. (2019, feb). A Scale to Characterize the Strength and Impacts of Atmospheric Rivers. *Bulletin of the American Meteorological Society*, 100(2), 269–289. Retrieved from <https://journals.ametsoc.org/bams/article/100/2/269/69196/A-Scale-to-Characterize-the-Strength-and-Impacts> doi: 10.1175/BAMS-D-18-0023.1
- Ralph, F. M., Wilson, A. M., Shulgina, T., Kawzenuk, B., Sellars, S., Rutz, J. J., ... Wick, G. A. (2019, apr). ARTMIP-early start comparison of atmospheric river detection tools: how many atmospheric rivers hit northern California’s Russian River watershed? *Climate Dynamics*, 52(7-8), 4973–4994. Retrieved from <https://doi.org/10.1007/s00382-018-4427-5>. <http://link.springer.com/10.1007/s00382-018-4427-5> doi: 10.1007/s00382-018-4427-5
- Rauber, R. M., Hu, H., Dominguez, F., Nesbitt, S. W., McFarquhar, G. M., Zaremba, T. J., & Finlon, J. A. (2020). Structure of an Atmospheric River Over Australia and the Southern Ocean. Part I: Tropical and Midlatitude Water Vapor Fluxes. *Journal of Geophysical Research: Atmospheres*, 125(18), 1–18. doi: 10.1029/2020JD032513
- Reid, K. J., O’Brien, T. A., King, A. D., & Lane, T. P. (2021, nov). Extreme Water Vapor Transport During the March 2021 Sydney Floods in the Context of Climate Projections. *Geophysical Research Letters*, 48(22), 1–8. Retrieved from <https://onlinelibrary.wiley.com/doi/10.1029/2021GL095335> doi: 10.1029/2021GL095335
- Rhoades, A. M., Jones, A. D., Srivastava, A., Huang, H., O’Brien, T. A., Patricola, C. M., ... Zhou, Y. (2020). The Shifting Scales of Western U.S. Landfalling Atmospheric Rivers Under Climate Change. *Geophysical Research Letters*, 47(17), 1–14. doi: 10.1029/2020GL089096
- Rutz, J. J., James Steenburgh, W., & Martin Ralph, F. (2014, feb). Climatological characteristics of atmospheric rivers and their inland penetration over the western united states. *Monthly Weather Review*, 142(2), 905–921. Retrieved from <https://journals.ametsoc.org/mwr/article/142/2/905/71947/Climatological-Characteristics-of-Atmospheric> doi: 10.1175/MWR-D-13-00168.1
- Rutz, J. J., Shields, C. A., Lora, J. M., Payne, A. E., Guan, B., Ullrich, P., ... Viale, M. (2019, dec). The Atmospheric River Tracking Method Inter-comparison Project (ARTMIP): Quantifying Uncertainties in Atmospheric River Climatology. *Journal of Geophysical Research: Atmospheres*, 124(24), 13777–13802. Retrieved from <https://onlinelibrary.wiley.com/doi/abs/10.1029/2019JD030936> doi: 10.1029/2019JD030936
- Ryoo, J. M., Kaspi, Y., Waugh, D. W., Kiladis, G. N., Waliser, D. E., Fetzer, E. J., & Kim, J. (2013). Impact of rossby wave breaking on U.S. west coast winter precipitation during ENSO events. *Journal of Climate*, 26(17), 6360–6382. doi: 10.1175/JCLI-D-12-00297.1
- Shaw, T. A. (2019). Mechanisms of Future Predicted Changes in the Zonal Mean Mid-Latitude Circulation. *Current Climate Change Reports*, 5(4), 345–357. doi: 10.1007/s40641-019-00145-8
- Shaw, T. A., Baldwin, M., Barnes, E. A., Caballero, R., Garfinkel, C. I., Hwang, Y. T., ... Voigt, A. (2016). Storm track processes and the opposing influences of climate change. *Nature Geoscience*, 9(9), 656–664. doi: 10.1038/ngeo2783

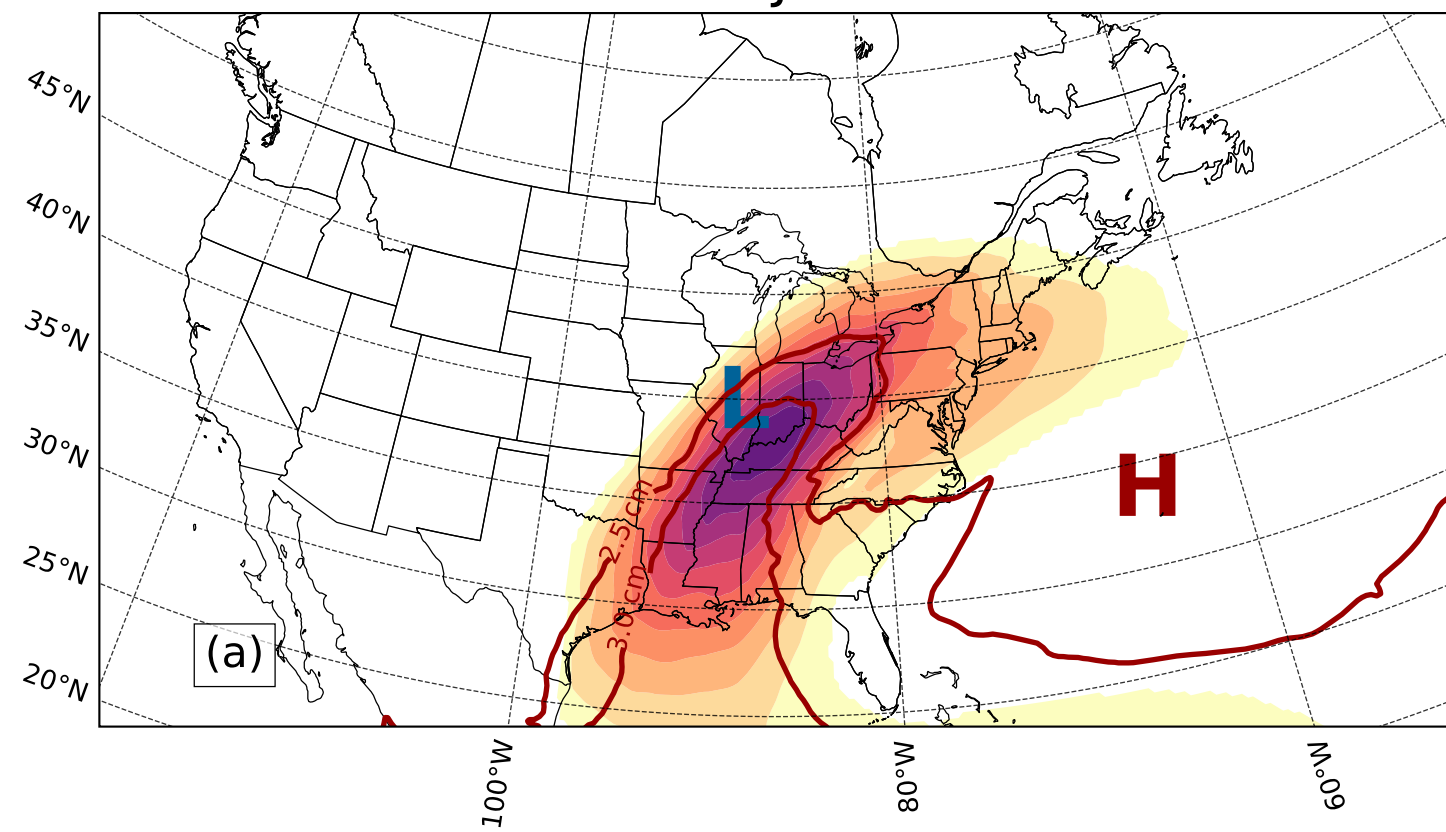
- Shields, C. A., Rutz, J. J., Leung, L.-Y., Ralph, F. M., Wehner, M., Kawzenuk, B., ... Nguyen, P. (2018, jun). Atmospheric River Tracking Method Intercomparison Project (ARTMIP): project goals and experimental design. *Geoscientific Model Development*, 11(6), 2455–2474. Retrieved from <https://www.geosci-model-dev.net/11/2455/2018/> doi: 10.5194/gmd-11-2455-2018
- Skinner, C. B., Lora, J. M., Payne, A. E., & Poulsen, C. J. (2020). Atmospheric river changes shaped mid-latitude hydroclimate since the mid-Holocene. *Earth and Planetary Science Letters*, 541, 116293. Retrieved from <https://doi.org/10.1016/j.epsl.2020.116293> doi: 10.1016/j.epsl.2020.116293
- Skinner, C. B., Lora, J. M., Tabor, C., & Zhu, J. (2023). Atmospheric River Contributions to Ice Sheet Hydroclimate at the Last Glacial Maximum. *Geophysical Research Letters*, 50(1), 1–12. doi: 10.1029/2022GL101750
- Slinsky, E. A., Loikith, P. C., Waliser, D. E., Guan, B., & Martin, A. (2020, nov). A Climatology of Atmospheric Rivers and Associated Precipitation for the Seven U.S. National Climate Assessment Regions. *Journal of Hydrometeorology*, 21(11), 2439–2456. Retrieved from <https://journals.ametsoc.org/view/journals/hydr/21/11/JHM-D-20-0039.1.xml> doi: 10.1175/JHM-D-20-0039.1
- Smith, B. L., Yuter, S. E., Neiman, P. J., & Kingsmill, D. E. (2010). Water vapor fluxes and orographic precipitation over northern california associated with a landfalling atmospheric river. *Monthly Weather Review*, 138(1), 74–100. doi: 10.1175/2009MWR2939.1
- Smith, L. M., & Stechmann, S. N. (2017). Precipitating quasigeostrophic equations and potential vorticity inversion with phase changes. *Journal of the Atmospheric Sciences*, 74(10), 3285–3303. doi: 10.1175/JAS-D-17-0023.1
- Sodemann, H., & Stohl, A. (2013). Moisture origin and meridional transport in atmospheric rivers and their association with multiple cyclones. *Monthly Weather Review*, 141(8), 2850–2868. doi: 10.1175/MWR-D-12-00256.1
- Stohl, A., Forster, C., & Sodemann, H. (2008). Remote sources of water vapor forming precipitation on the Norwegian west coast at 60°N - A tale of hurricanes and an atmospheric river. *Journal of Geophysical Research Atmospheres*, 113(5), 1–13. Retrieved from <http://dx.doi.org/10.1029/2007JD009006> doi: 10.1029/2007JD009006
- Strong, C., & Magnusdottir, G. (2008a). How Rossby wave breaking over the Pacific forces the North Atlantic Oscillation. *Geophysical Research Letters*, 35(10), 1–5. doi: 10.1029/2008GL033578
- Strong, C., & Magnusdottir, G. (2008b, sep). Tropospheric Rossby Wave Breaking and the NAO/NAM. *Journal of the Atmospheric Sciences*, 65(9), 2861–2876. Retrieved from <https://journals.ametsoc.org/jas/article/65/9/2861/26245/Tropospheric-Rossby-Wave-Breaking-and-the-NAONAM> doi: 10.1175/2008JAS2632.1
- Sun, C., Shanahan, T. M., DiNezio, P. N., McKay, N. P., & Roy, P. D. (2021). Great Plains storm intensity since the last glacial controlled by spring surface warming. *Nature Geoscience*, 14(12), 912–917. doi: 10.1038/s41561-021-00860-8
- Viale, M., & Nuñez, M. N. (2011). Climatology of winter orographic precipitation over the subtropical central Andes and associated synoptic and regional characteristics. *Journal of Hydrometeorology*, 12(4), 481–507. doi: 10.1175/2010JHM1284.1
- Waliser, D., & Guan, B. (2017, mar). Extreme winds and precipitation during landfall of atmospheric rivers. *Nature Geoscience*, 10(3), 179–183. Retrieved from <https://doi.org/10.1038/ngeo2894> <http://www.nature.com/articles/ngeo2894> doi: 10.1038/ngeo2894
- Warner, M. D., & Mass, C. F. (2017, aug). Changes in the climatology, struc-

- ture, and seasonality of northeast pacific atmospheric rivers in CMIP5 climate simulations. *Journal of Hydrometeorology*, 18(8), 2131–2141. Retrieved from <http://journals.ametsoc.org/doi/10.1175/JHM-D-16-0200.1> doi: 10.1175/JHM-D-16-0200.1
- Warner, M. D., Mass, C. F., & Salathé, E. P. (2015). Changes in Winter Atmospheric Rivers along the North American West Coast in CMIP5 Climate Models. *Journal of Hydrometeorology*, 16(1), 118–128. Retrieved from <http://journals.ametsoc.org/doi/10.1175/JHM-D-14-0080.1> doi: 10.1175/JHM-D-14-0080.1
- Warner, M. D., Mass, C. F., & Salathé, E. P. (2012). Wintertime extreme precipitation events along the Pacific Northwest Coast: Climatology and synoptic evolution. *Monthly Weather Review*, 140(7), 2021–2043. doi: 10.1175/MWR-D-11-00197.1
- Wille, J. D., Favier, V., Dufour, A., Gorodetskaya, I. V., Turner, J., Agosta, C., & Codron, F. (2019). West Antarctic surface melt triggered by atmospheric rivers. *Nature Geoscience*, 12(11), 911–916. Retrieved from <http://dx.doi.org/10.1038/s41561-019-0460-1> doi: 10.1038/s41561-019-0460-1
- Xu, L., Zhang, H., He, W., Ye, C., Moise, A., & Rodríguez, J. M. (2020). Potential connections between atmospheric rivers in China and Australia. *Journal of Southern Hemisphere Earth Systems Science*. Retrieved from <http://www.publish.csiro.au/?paper=ES19027> doi: 10.1071/ES19027
- Xu, Y., Zhang, H., Liu, Y., Han, Z., & Zhou, B. (2020). Atmospheric rivers in the Australia–Asian region under current and future climate in CMIP5 models. *Journal of Southern Hemisphere Earth Systems Science*. doi: 10.1071/es19044
- Zhang, H., Ye, C., & Moise, A. (2020). Atmospheric Rivers in the Australia–Asian Region: A BoM–CMA Collaborative Study. *Journal of Southern Hemisphere Earth Systems Science*(January), 73. Retrieved from <https://drive.google.com/file/d/1EbLLO9SRtnu0etnB5PwJ6xRrQtU-U2D0/view> doi: 10.1071/ES19025
- Zhang, Z., Ralph, F. M., & Zheng, M. (2019, feb). The Relationship Between Extratropical Cyclone Strength and Atmospheric River Intensity and Position. *Geophysical Research Letters*, 46(3), 1814–1823. Retrieved from <https://onlinelibrary.wiley.com/doi/abs/10.1029/2018GL079071> doi: 10.1029/2018GL079071
- Zheng, M., Delle Monache, L., Cornuelle, B. D., Ralph, F. M., Tallapragada, V. S., Subramanian, A., ... DeHaan, L. (2021). Improved Forecast Skill Through the Assimilation of Dropsonde Observations From the Atmospheric River Reconnaissance Program. *Journal of Geophysical Research: Atmospheres*, 126(21). doi: 10.1029/2021JD034967
- Zhou, Y., Kim, H., & Guan, B. (2018). Life Cycle of Atmospheric Rivers: Identification and Climatological Characteristics. *Journal of Geophysical Research: Atmospheres*, 123(22), 12,715–12,725. doi: 10.1029/2018JD029180
- Zhou, Y., & Kim, H.-M. (2018, sep). Prediction of atmospheric rivers over the North Pacific and its connection to ENSO in the North American multi-model ensemble (NMME). *Climate Dynamics*, 51(5-6), 1623–1637. Retrieved from <http://dx.doi.org/10.1007/s00382-017-3973-6> <http://link.springer.com/10.1007/s00382-017-3973-6> doi: 10.1007/s00382-017-3973-6
- Zhou, Y., O'Brien, T. A., Ullrich, P. A., Collins, W. D., Patricola, C. M., & Rhoades, A. M. (2021, apr). Uncertainties in Atmospheric River Life-cycles by Detection Algorithms: Climatology and Variability. *Journal of Geophysical Research: Atmospheres*, 126(8), 1–22. Retrieved from <https://onlinelibrary.wiley.com/doi/10.1029/2020JD033711> doi: 10.1029/2020JD033711
- Zhu, Y., & Newell, R. E. (1994, sep). Atmospheric rivers and bombs. *Geophysical*

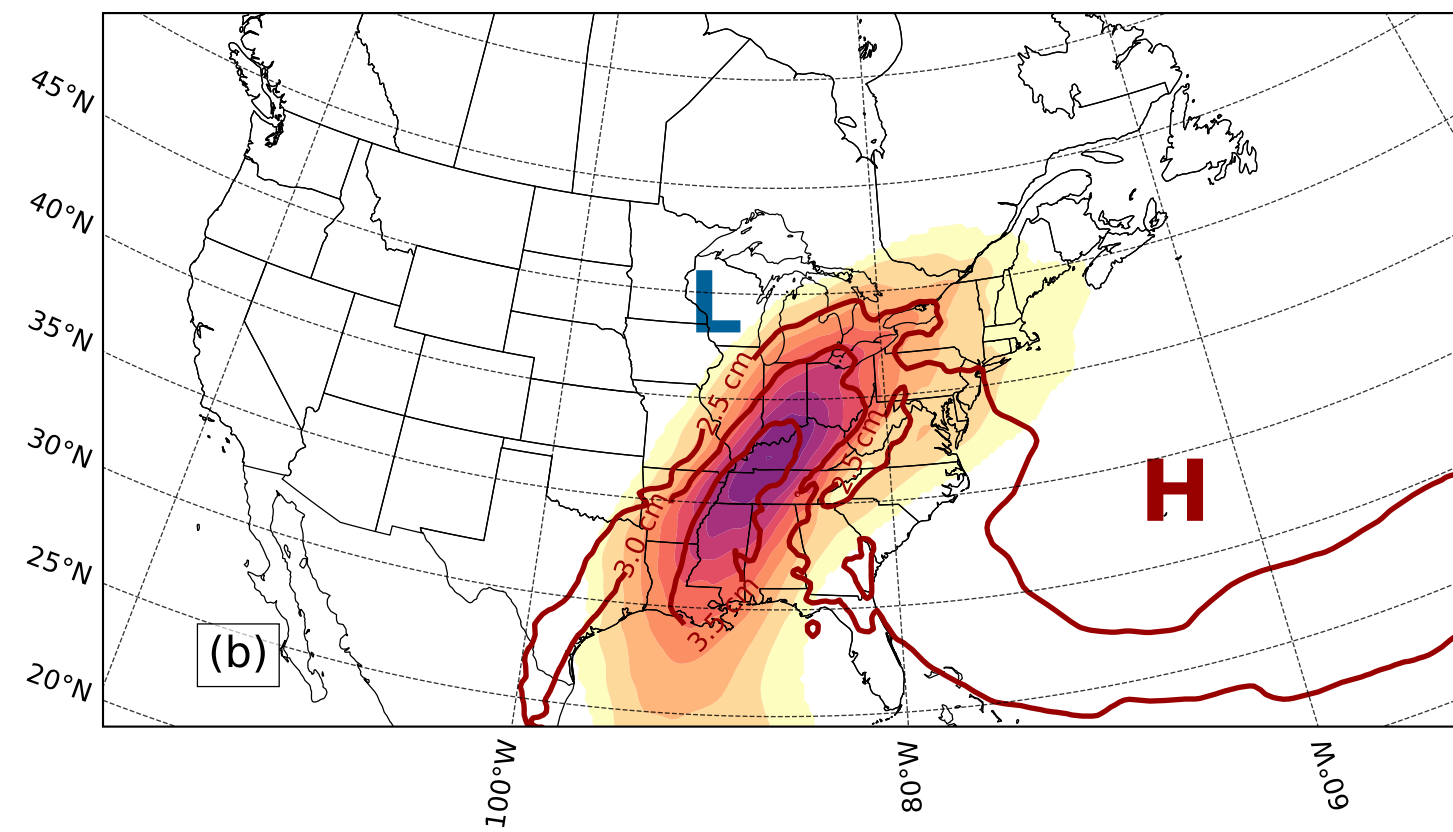
888 *Research Letters*, 21(18), 1999–2002. Retrieved from [http://doi.wiley.com/](http://doi.wiley.com/10.1029/94GL01710)
889 10.1029/94GL01710 doi: 10.1029/94GL01710
890 Zhu, Y., & Newell, R. E. (1998, mar). A Proposed Algorithm for Moisture
891 Fluxes from Atmospheric Rivers. *Monthly Weather Review*, 126(3),
892 725–735. Retrieved from [http://journals.ametsoc.org/doi/abs/](http://journals.ametsoc.org/doi/abs/10.1175/1520-0493%281998%29126%3C0725%3AAPAFMF%3E2.0.CO%3B2)
893 10.1175/1520-0493(1998)126<0725:APA FMF>2.0.CO;2 doi:
894 10.1175/1520-0493(1998)126<0725:APA FMF>2.0.CO;2

Figure 1.

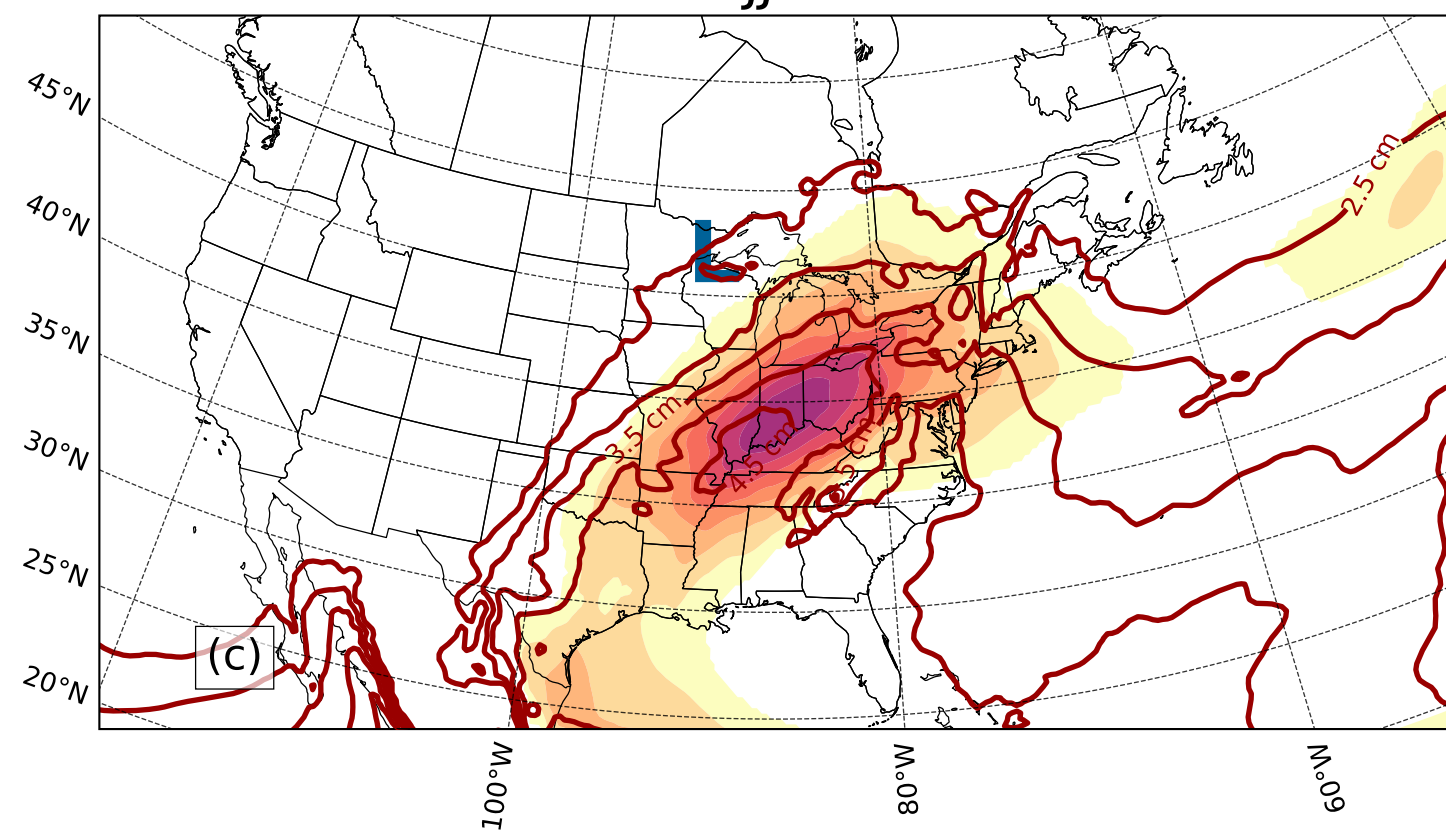
DJF



MAM



JJA



SON

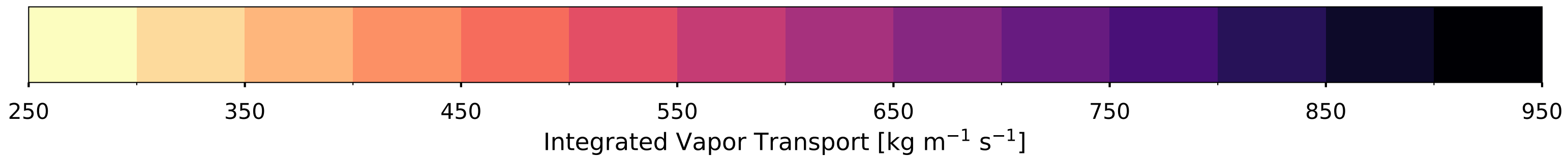
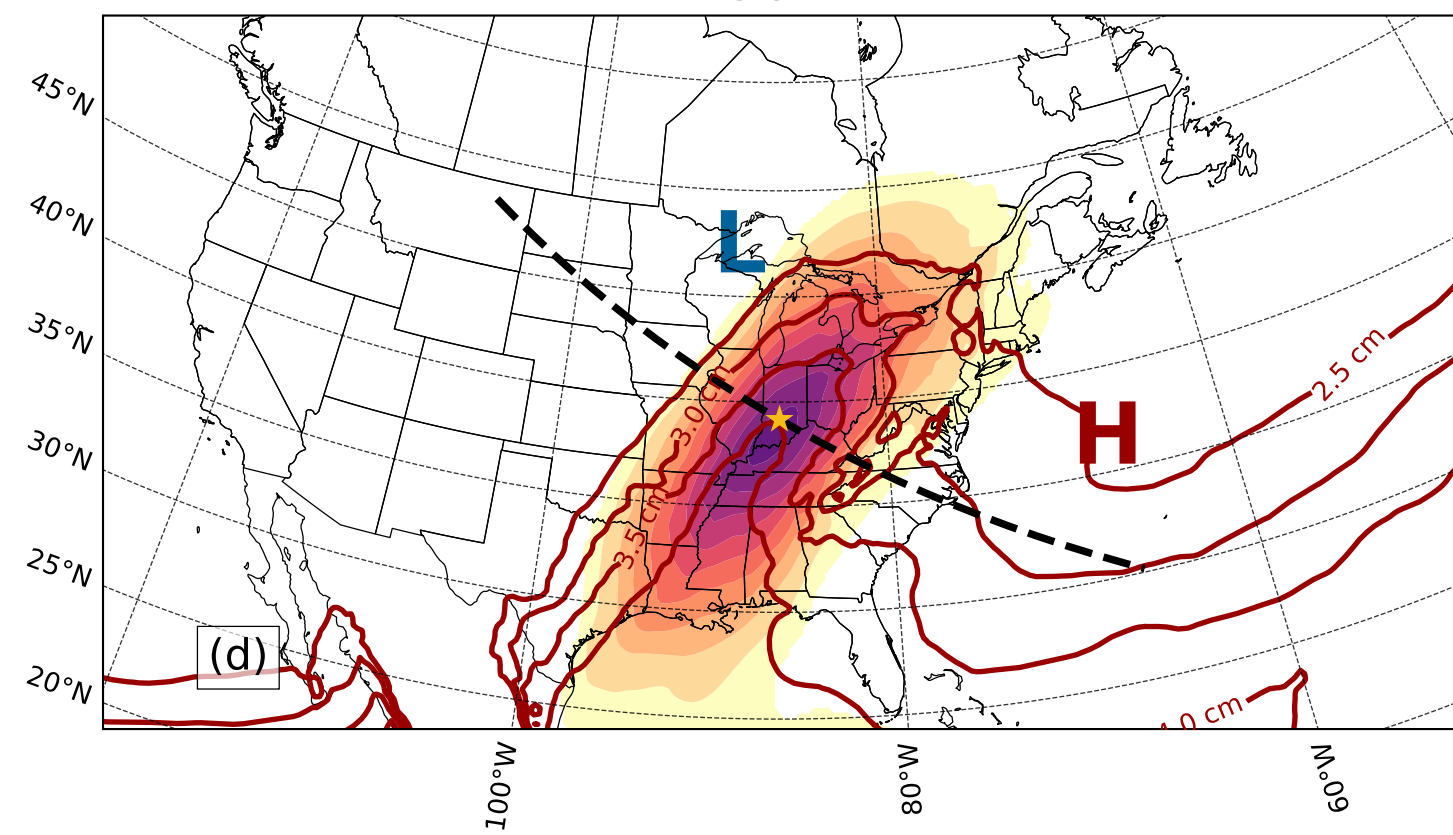
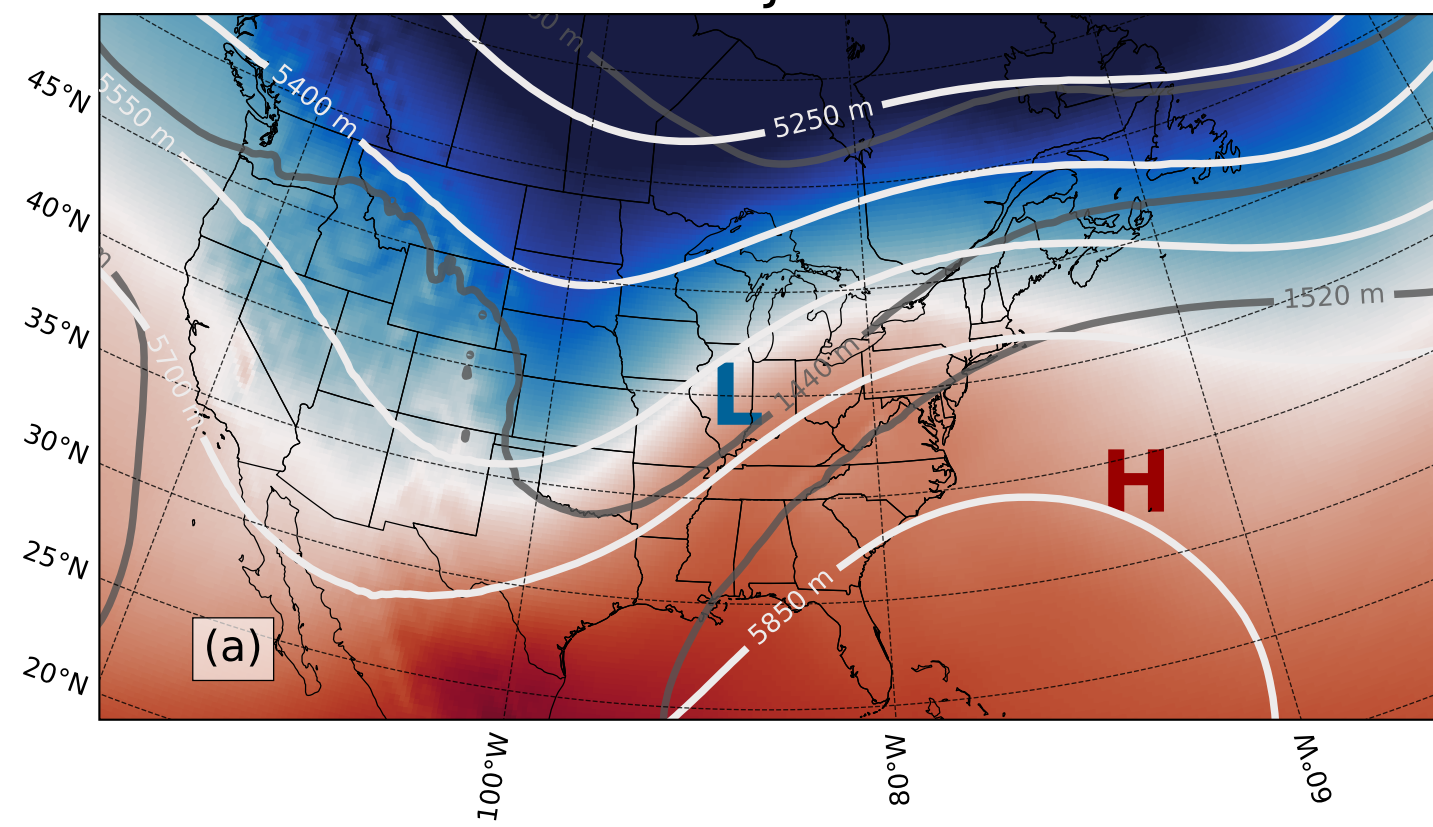
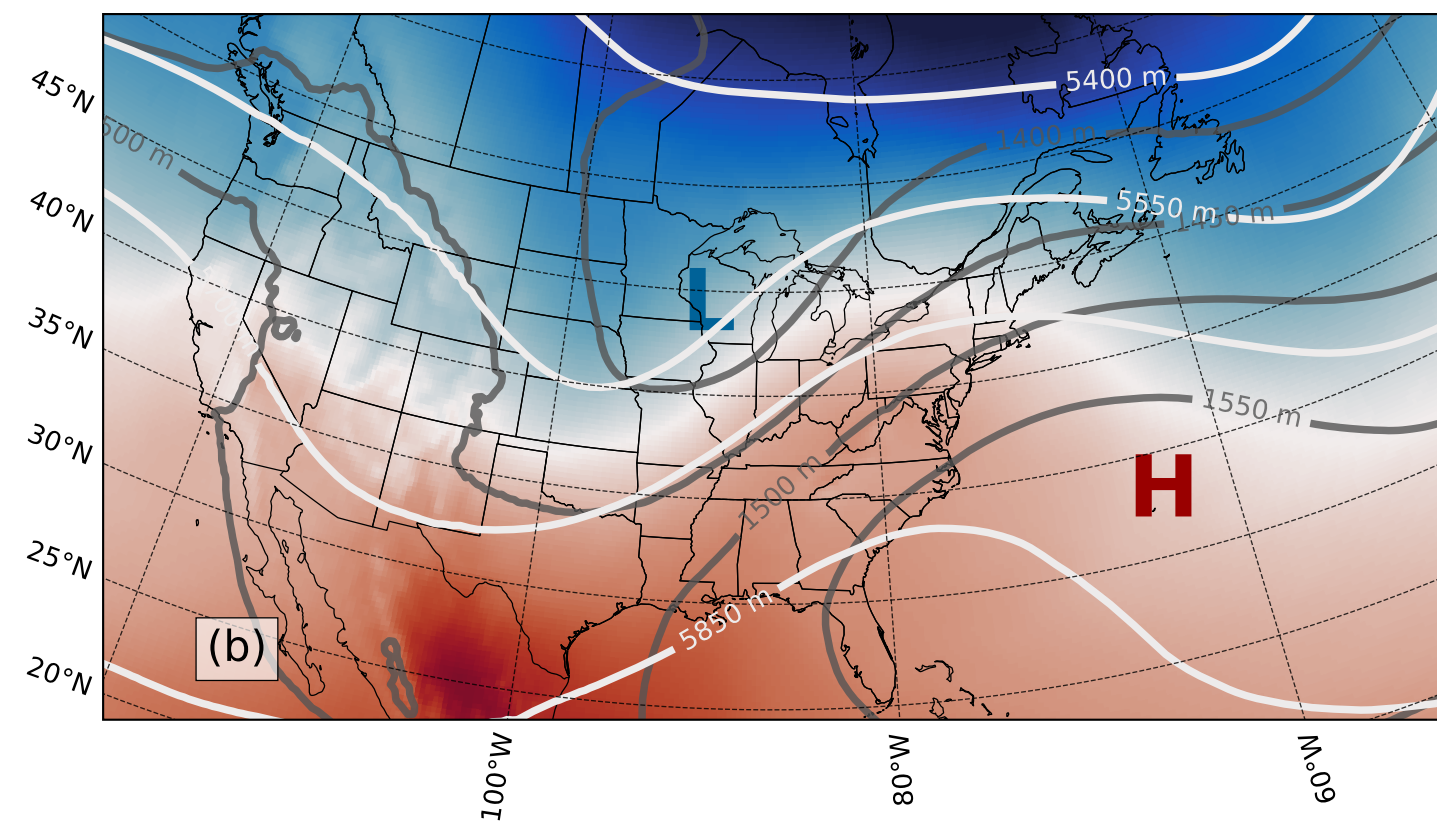


Figure 2.

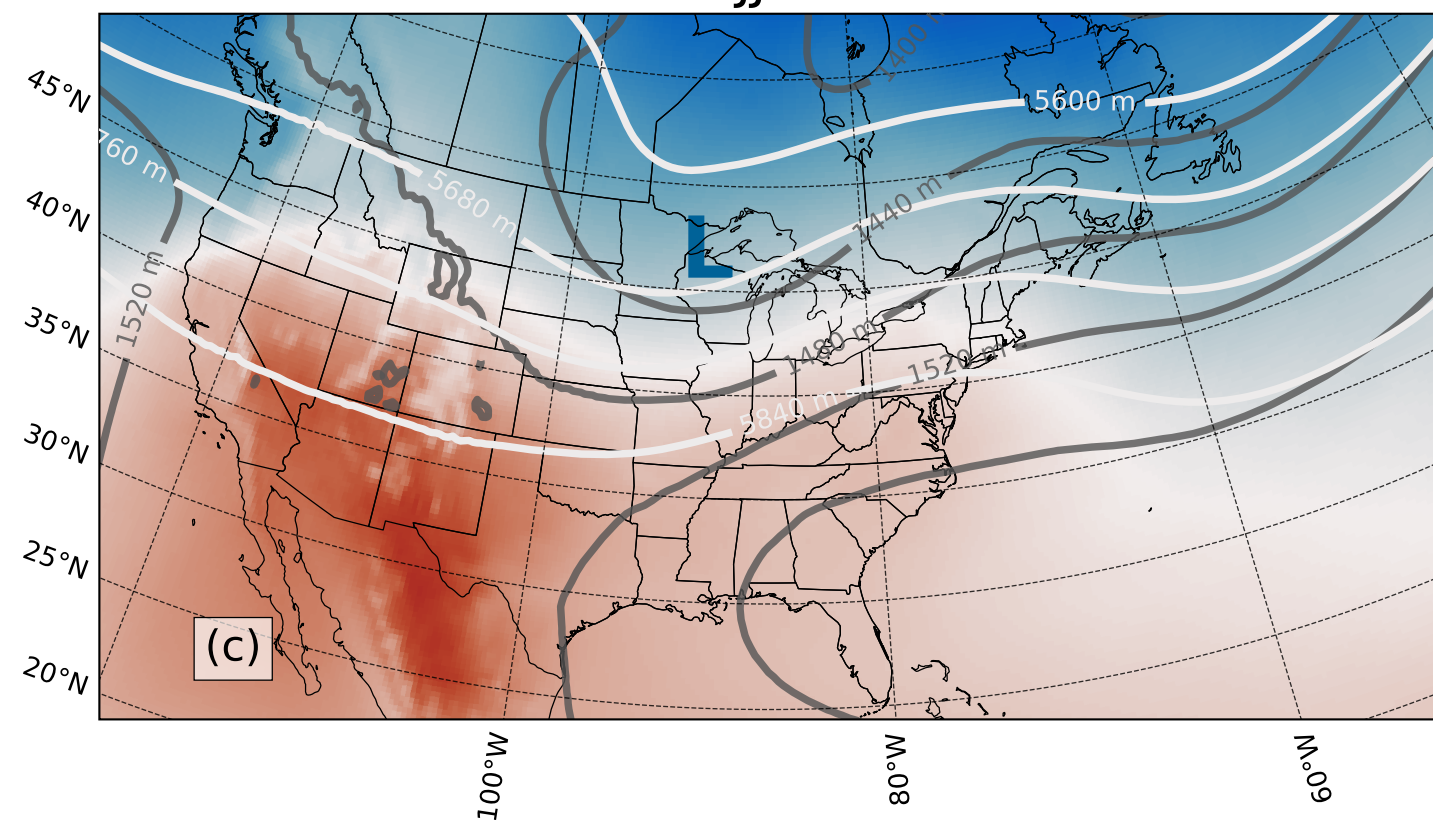
DJF



MAM



JJA



SON

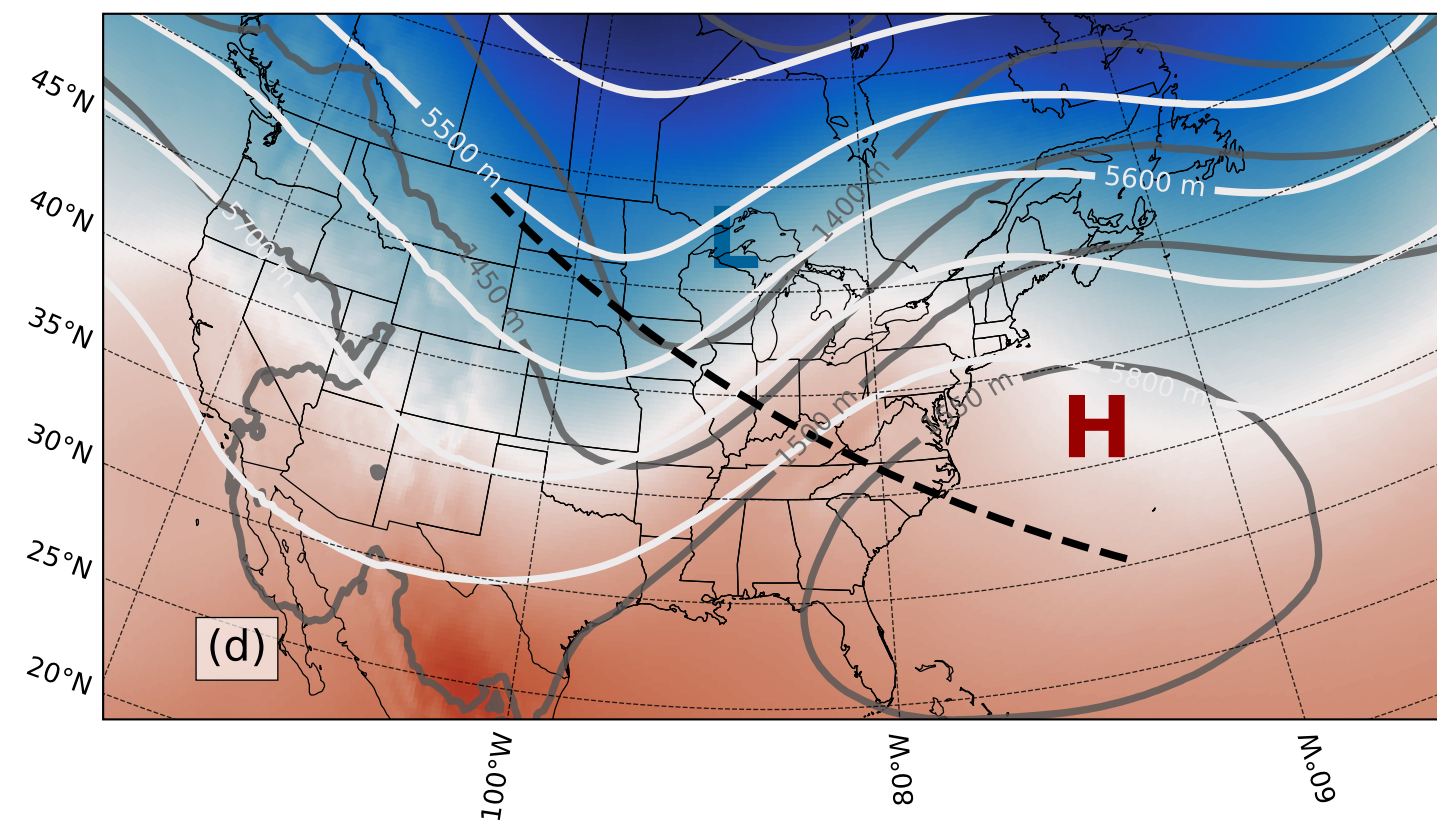


Figure 3.

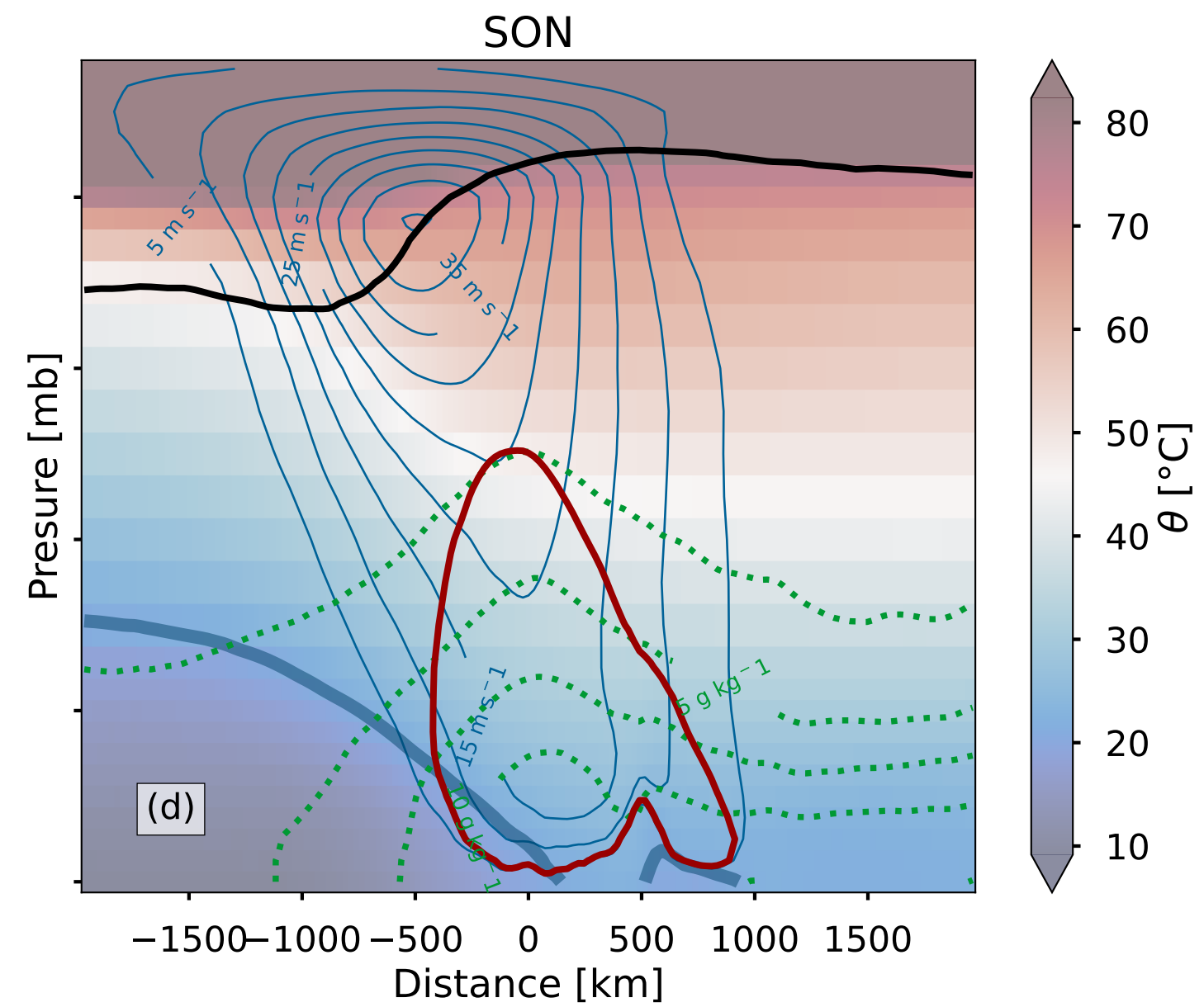
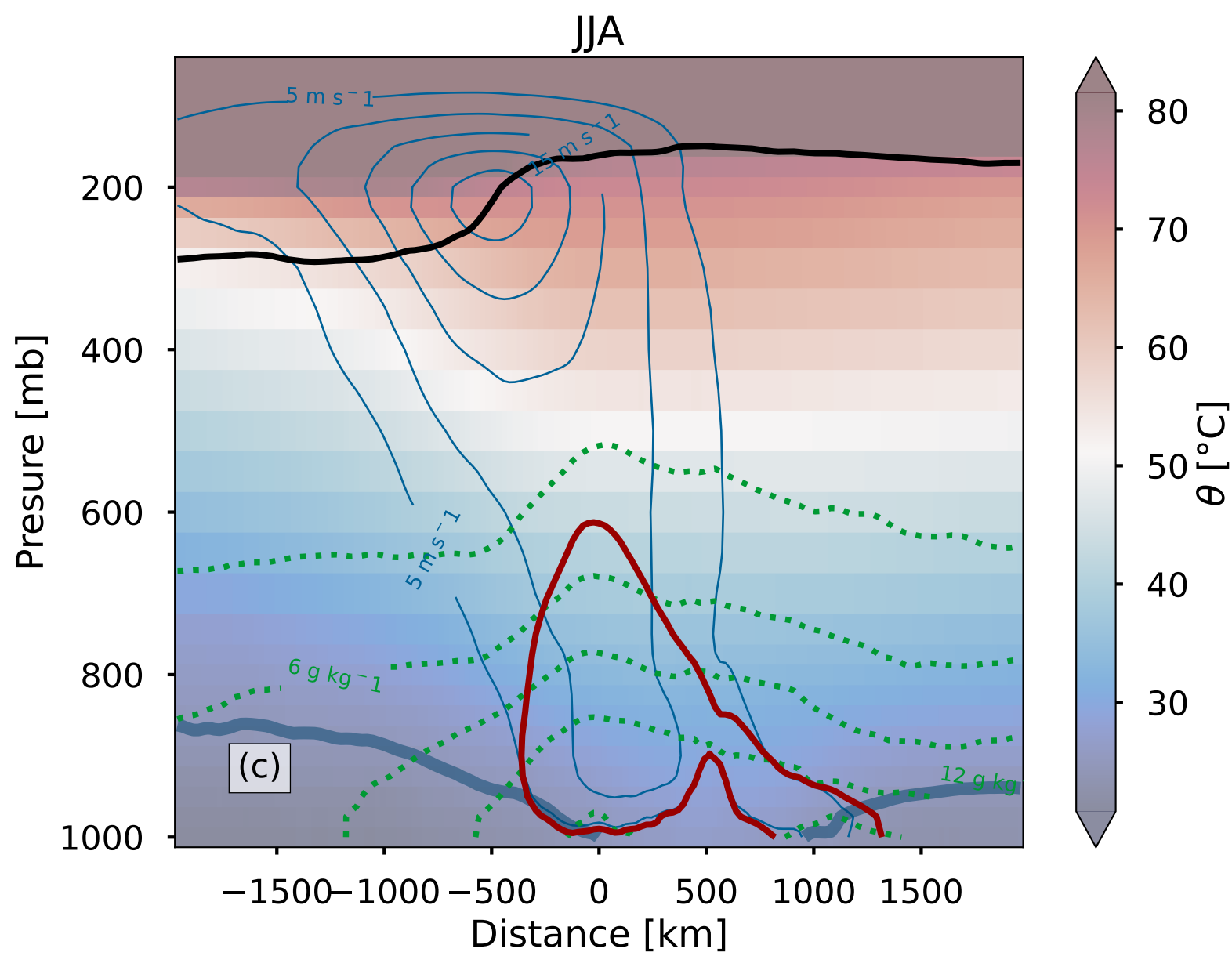
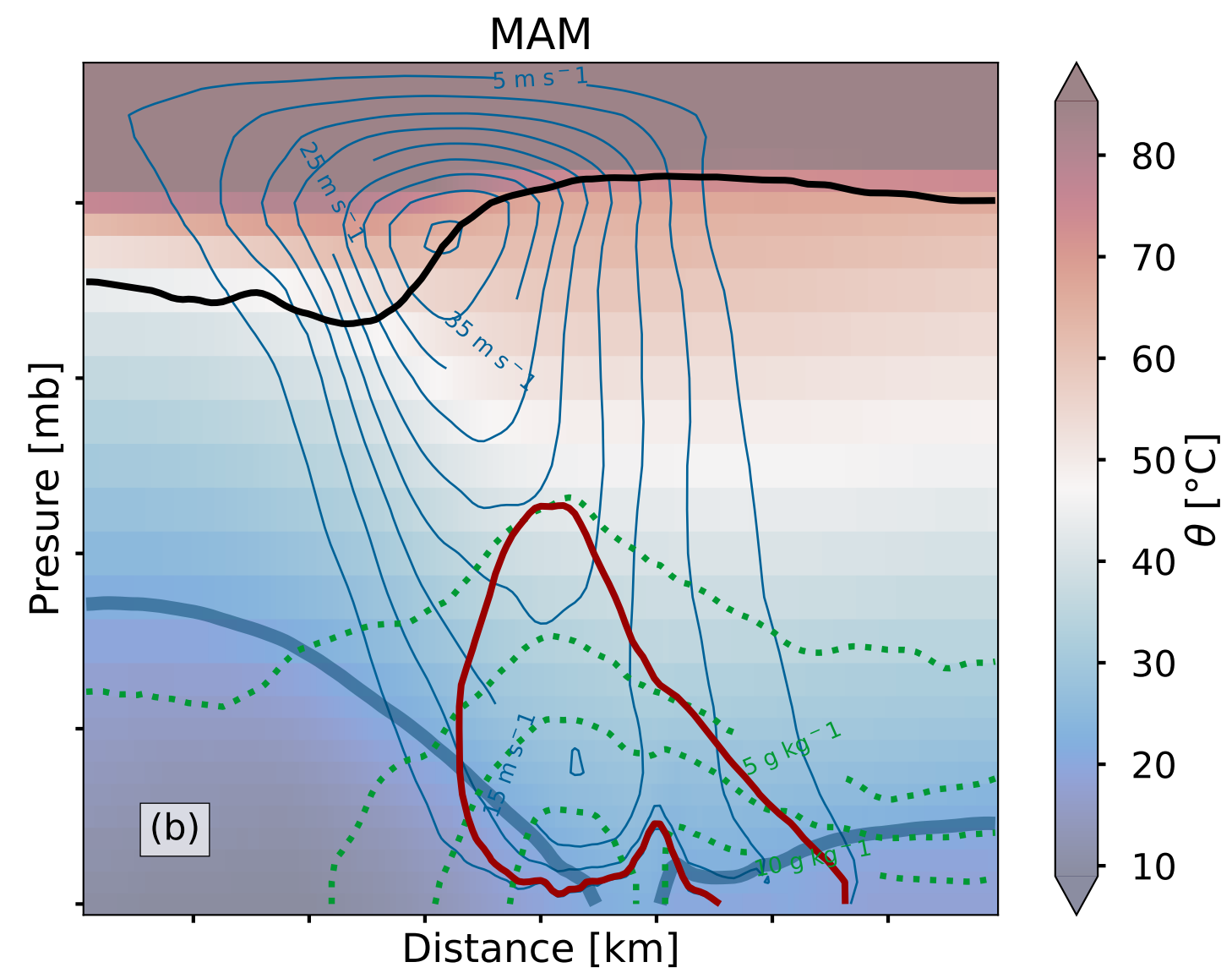
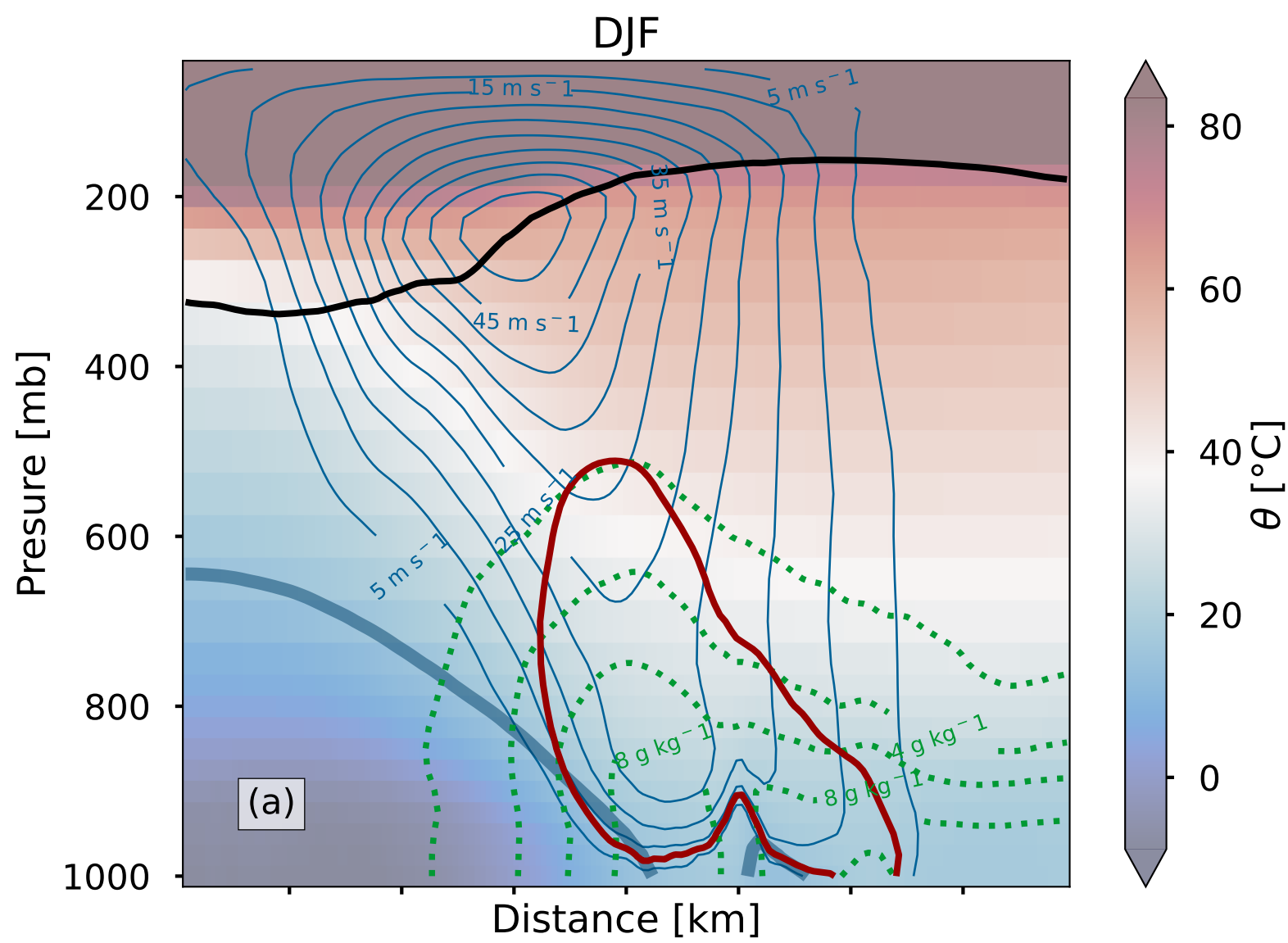
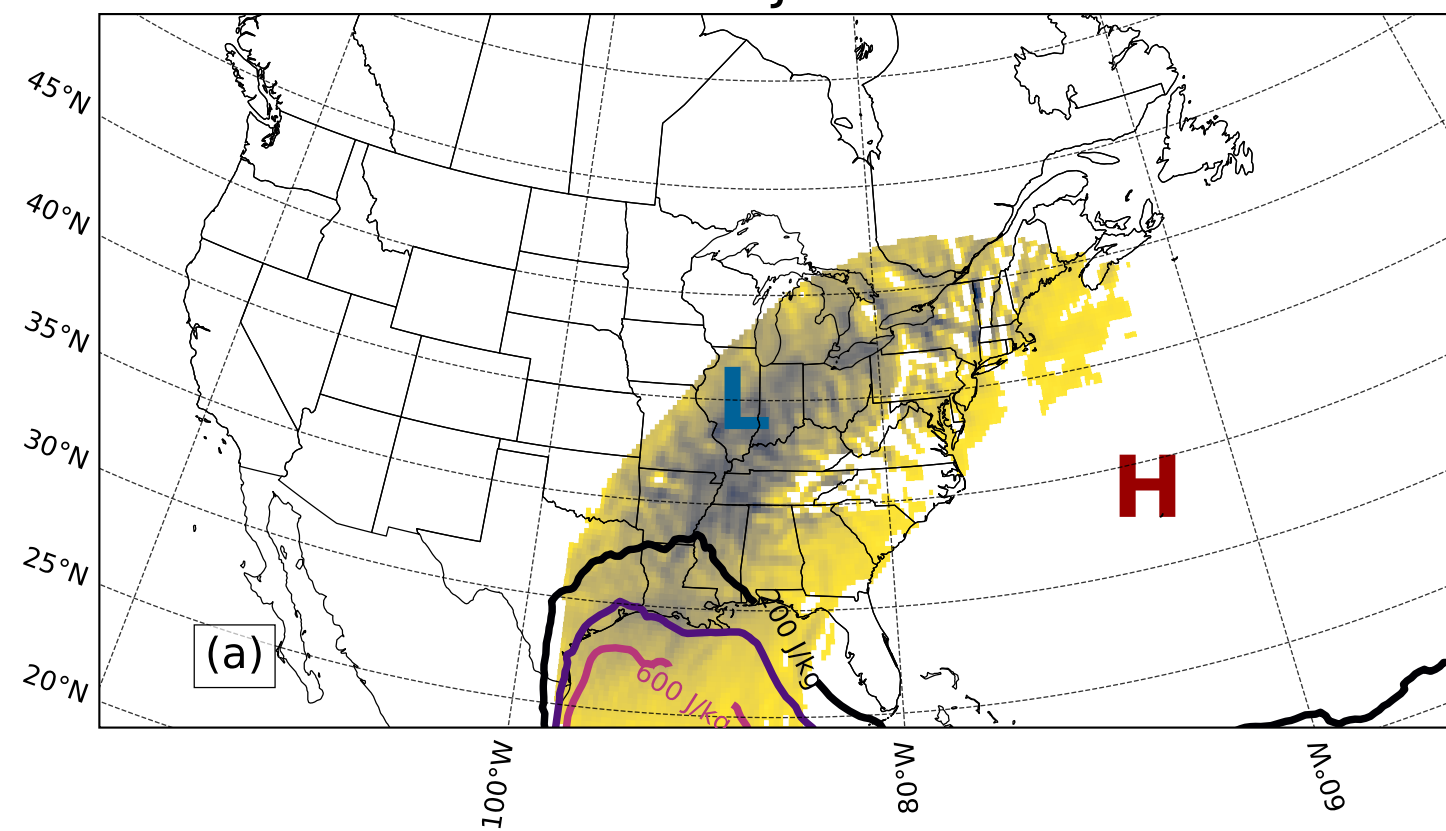
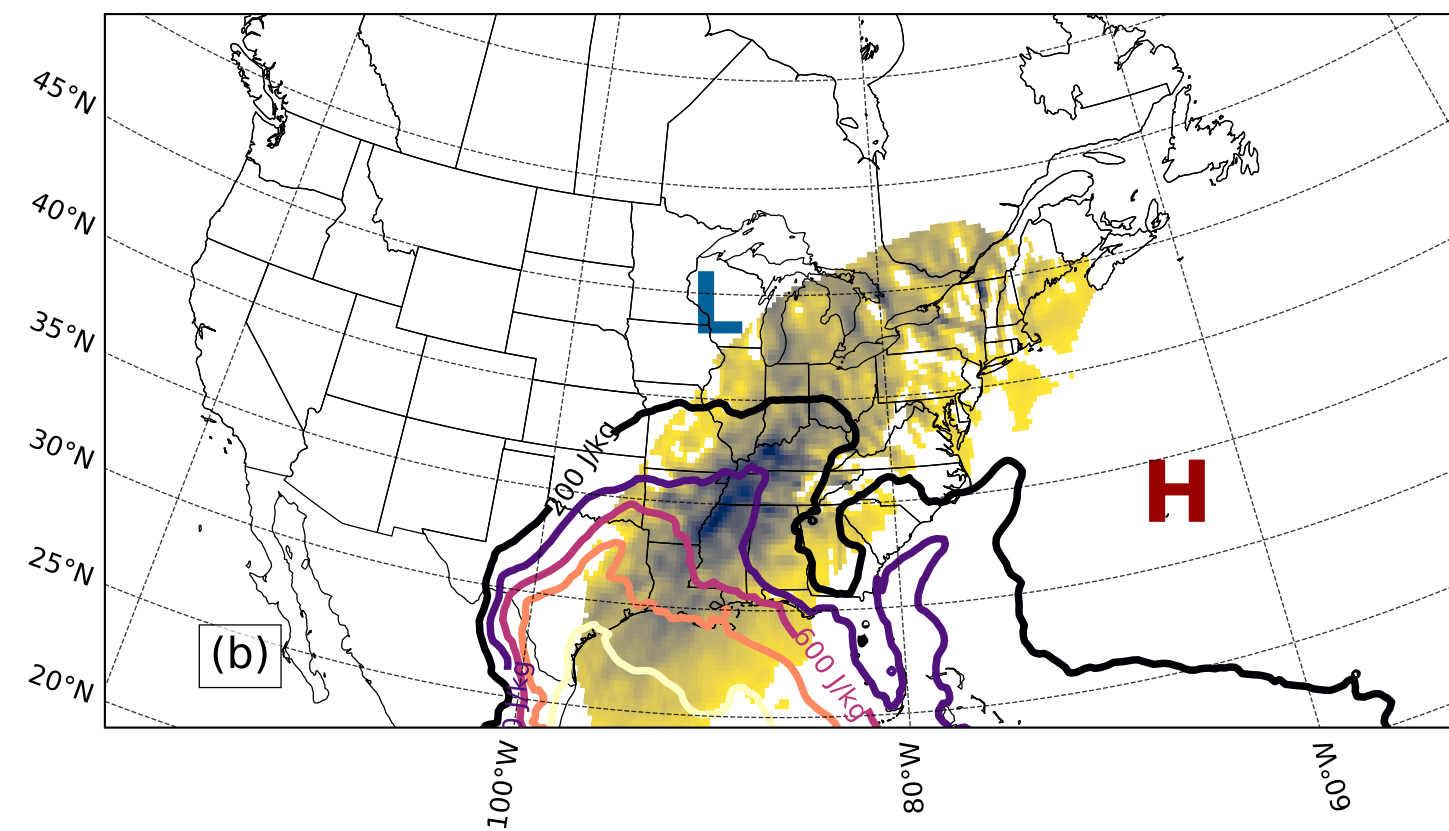


Figure 4.

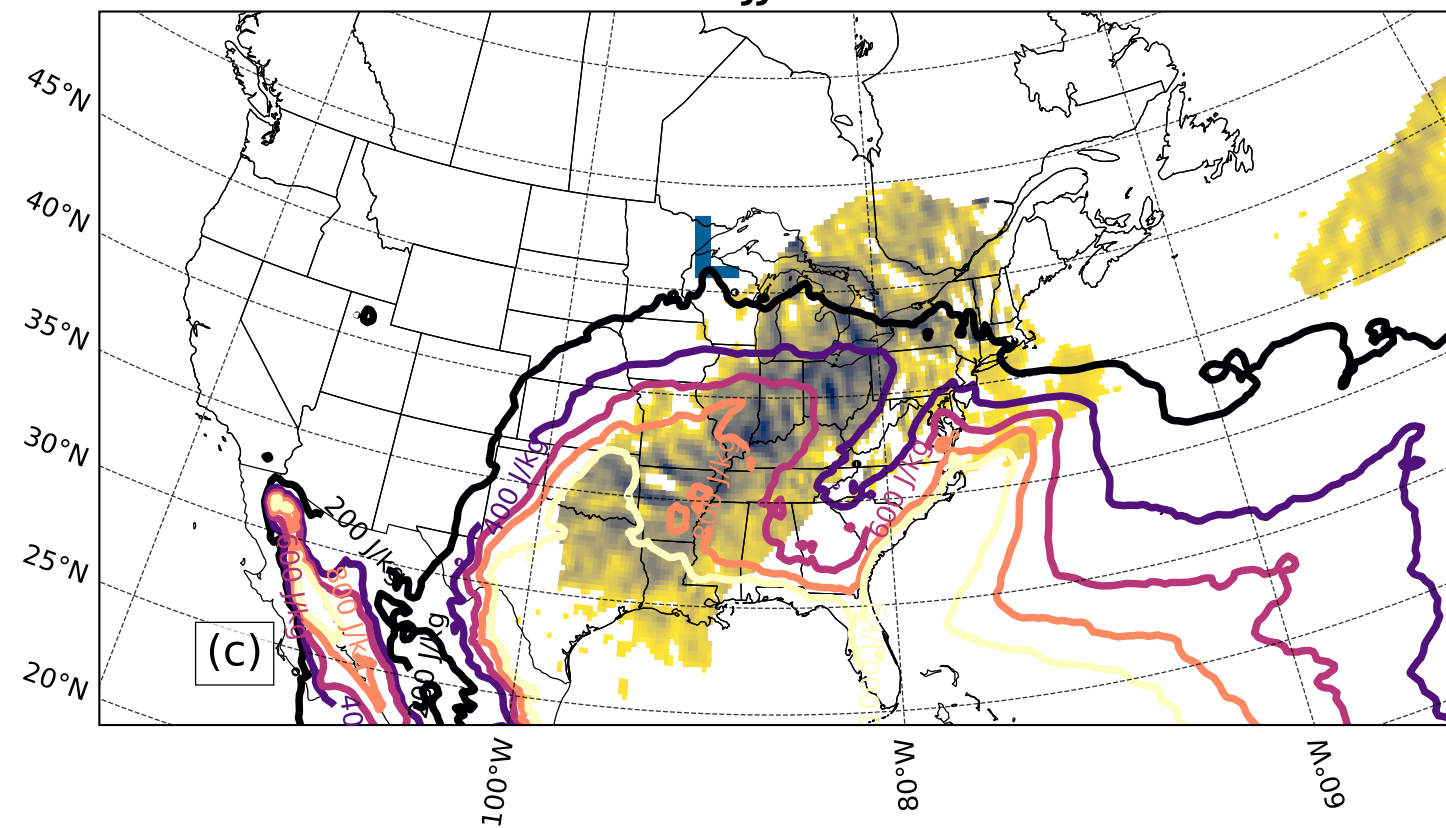
DJF



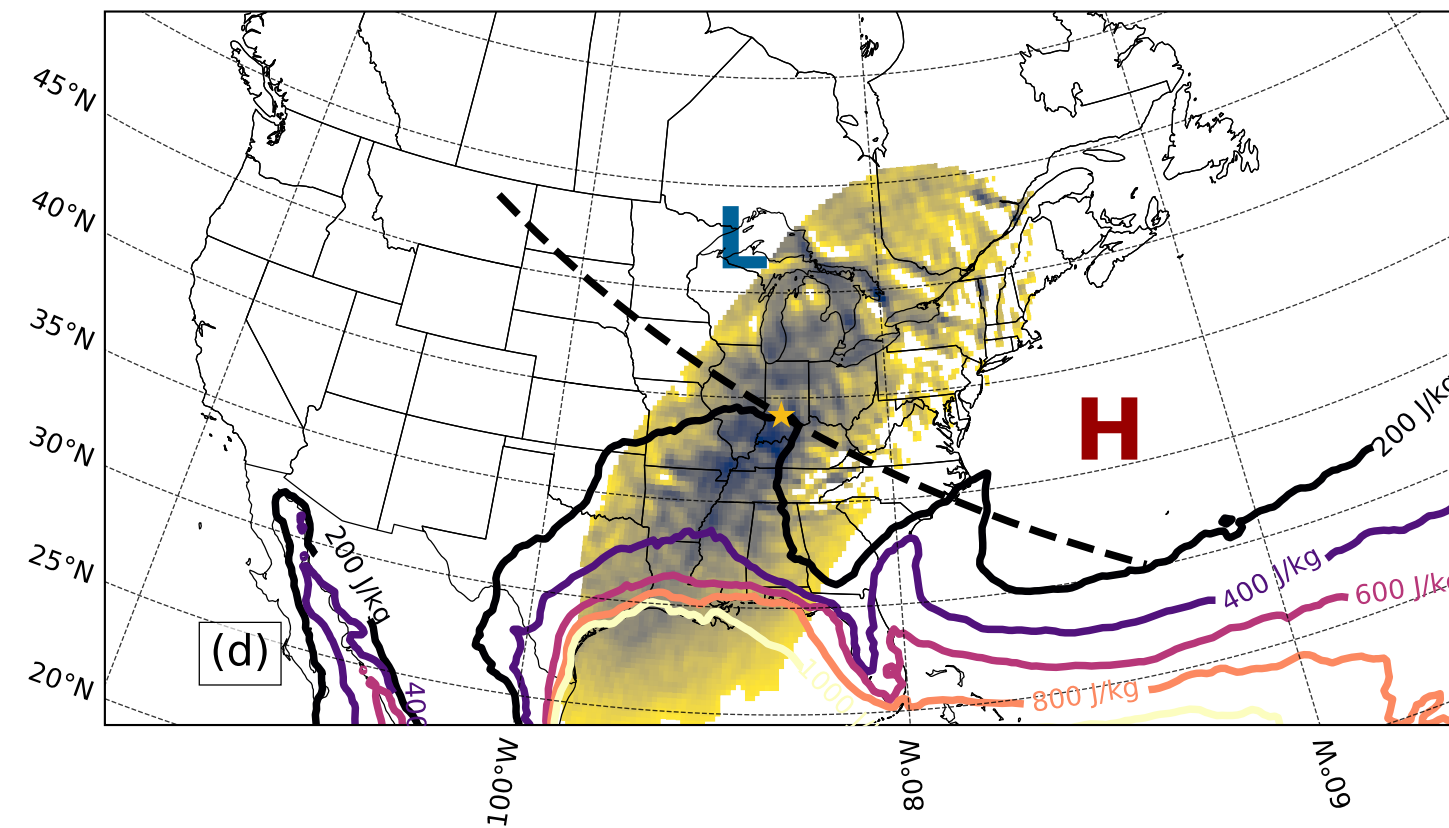
MAM



JJA



SON



-0.35

-0.30

-0.25

-0.20

-0.15

-0.10

-0.05

Vertical Velocity at 700 hPa [hPa/s]

Travis A. O'Brien,^{1,2}Burlen Loring,³Amanda Dufek,⁴Mohammad Rubaiat

Islam,¹Diya Kamnani,¹Kwesi Quagraine¹,Cody Kirkpatrick¹

¹Department of Earth and Atmospheric Sciences, Indiana University, Bloomington, IN,
²Climate and Cosystem Sciences Division, Lawrence Berkeley National Laboratory,
³Computational Research Division, Lawrence Berkeley National Laboratory,
⁴National Energy Research Supercomputing Center, Lawrence Berkeley National Laboratory

1. Figures S1 to S9

This supporting information file provides (1) a satellite overview of a specific Midwestern US AR event discussed in the introduction and discussion sections, provided to give context for those unfamiliar with the event; and (2) duplicates of Figure 1{4 in the main that show the sensitivity of the composites to choice of atmospheric river detection tool (ARDT) and to the choice of location on which the composites are centered.

Tan, J., Hu man, G. J., Bolvin, D. T., & Nelkin, E. J. (2019, dec). IMERG V06:

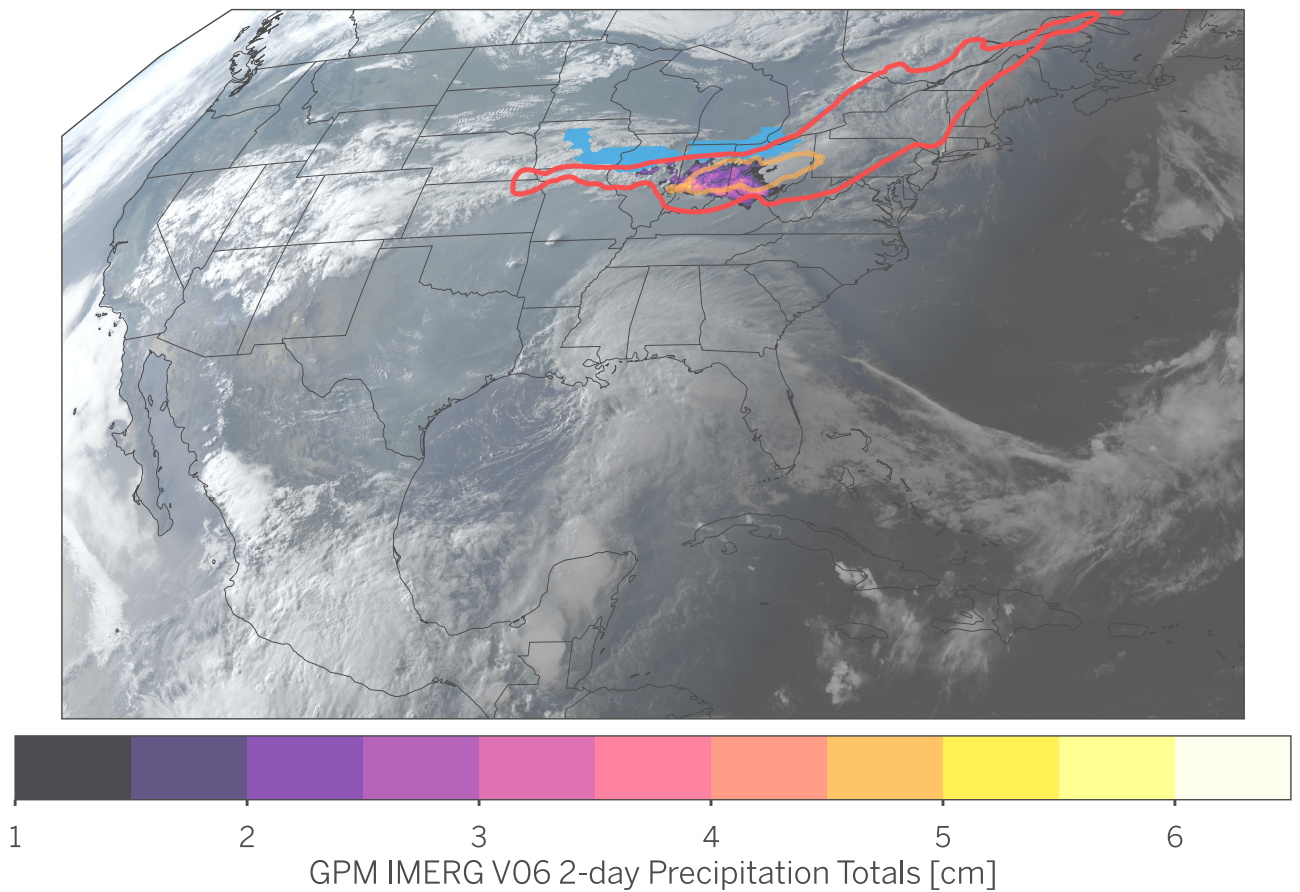
Changes to the Morphing Algorithm. ~~WFO~~

~~9~~, 8 (12), 2471{2482. Retrieved from ~~h~~

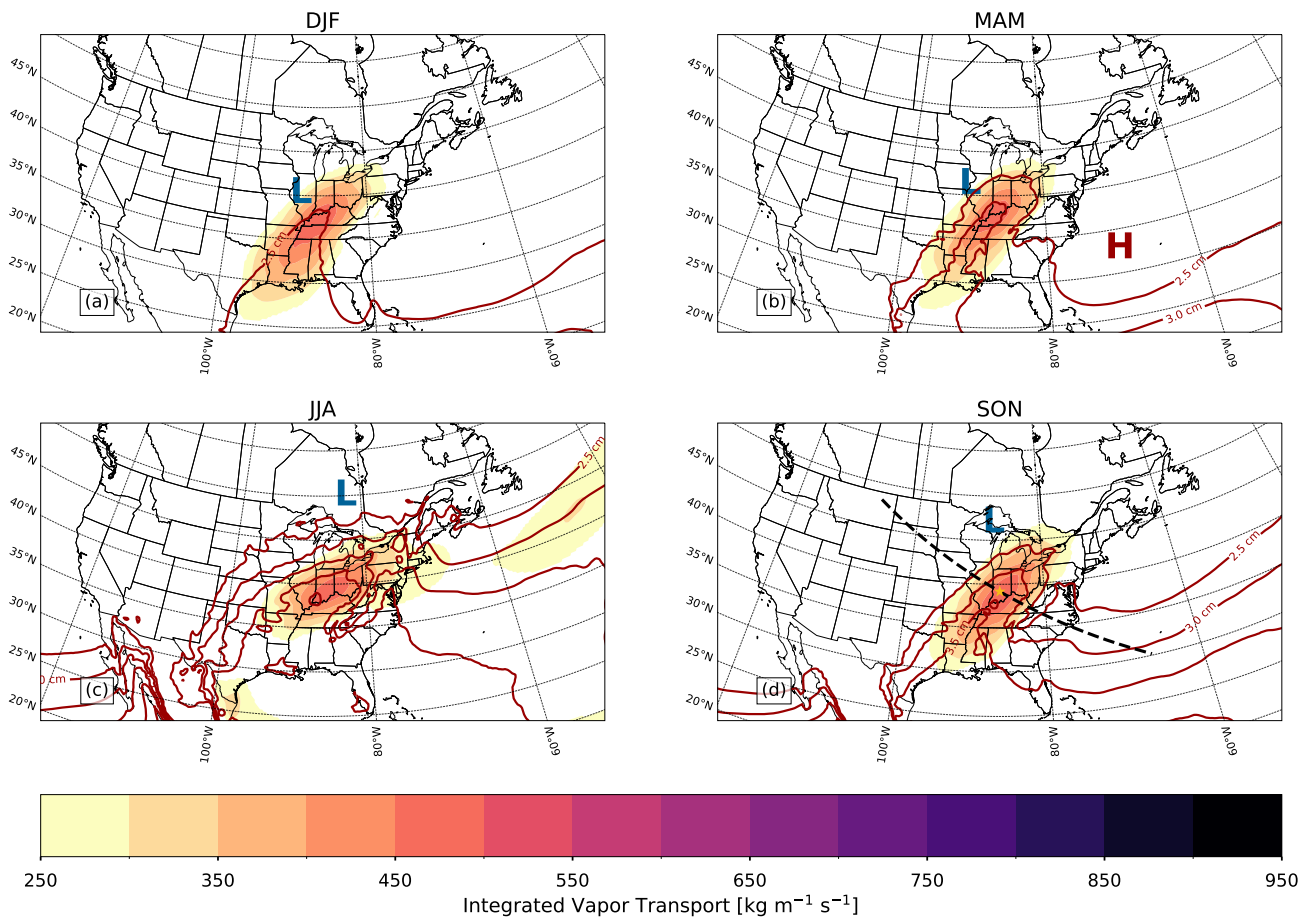
~~h~~

doi: 10.1175/JTECH-D-19-0114

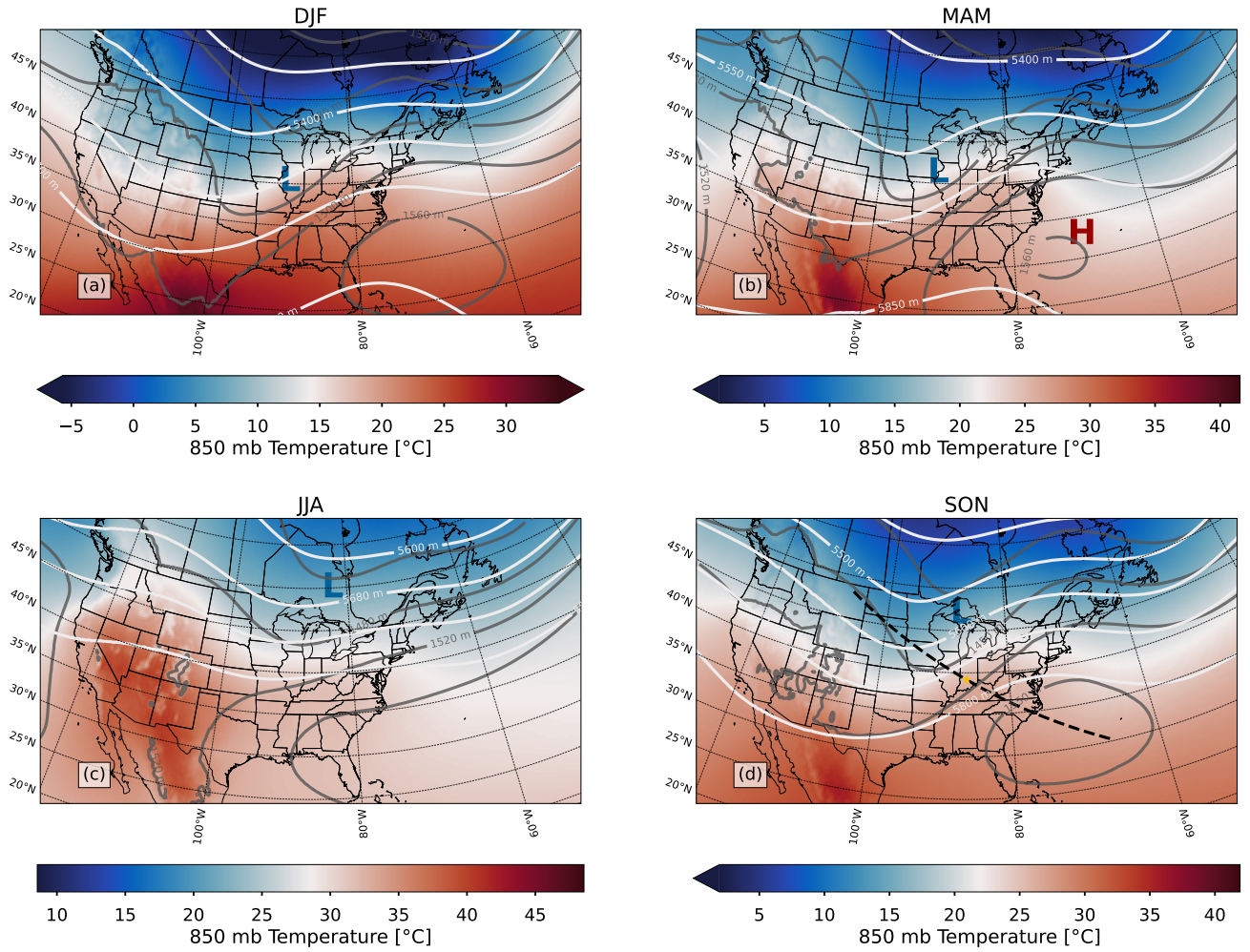
.1



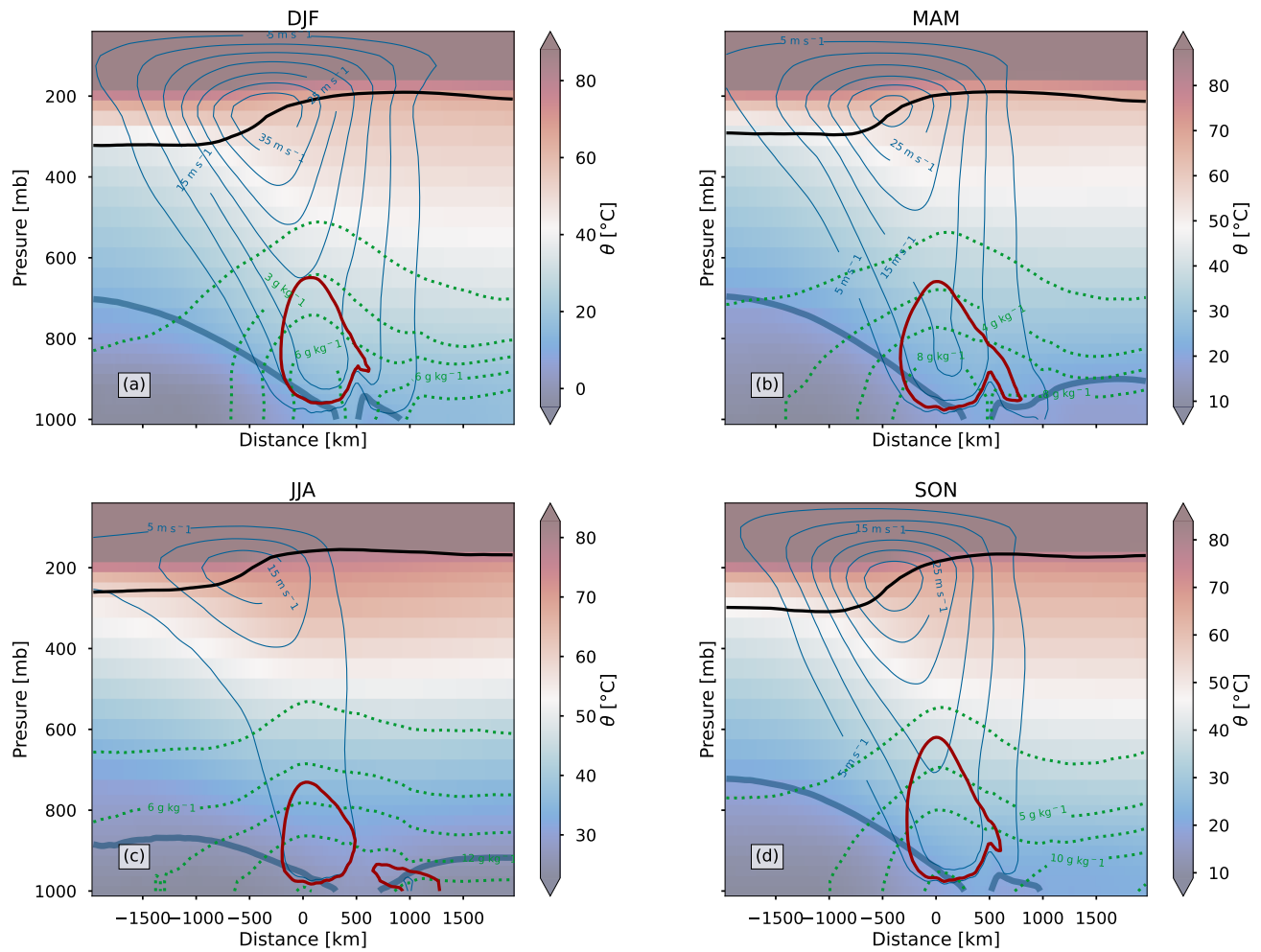
1 An objectively-detected frontal zone (blue shading), mesoscale convective complex (orange contour) and AR (red contour), detected in ERA5, overlain on geostationary satellite imagery from 03 UTC on June 19, 2021. Two-day precipitation totals from Global Precipitation Measurement mission (GPM) IMERG V06B (Tan et al., 2019), associated with this event, are shown as shaded contours.



2 As in Figure 1, but using the guanwaliser ARDT and centered on Bloomington, IN.



3 As in Figure 2, but using the guanwaliser ARDT and centered on Bloomington, IN.



4 As in Figure 3, but using the guanwaliser ARDT and centered on Bloomington,

IN.

Figure S5. As in Figure 4, but using the guanwaliser ARDT and centered on Bloomington, IN.

November 9, 2023, 6:57am